UCLouvain

AGRO LOUVAIN

Faculté des bioingénieurs

Towards the identification of ZmNAC24 transcription factor targets using DNA affinity purification sequencing in maize

Auteur Jean FONTAINE

Promoteurs Pr François CHAUMONT

Estelle TEIRLINCKX

Lecteurs Pr Frédéric CLOTMAN

Dr Alice BERHIN

Année académique 2022-2023

Mémoire de fin d'études présenté en vue de l'obtention du diplôme de Bioingénieur : chimie et bio-industrie

UNIVERSITÉ CATHOLIQUE DE LOUVAIN

Faculté des bioingénieurs

Master thesis

Towards the identification of ZmNAC24 transcription factor targets using DNA affinity purification sequencing in maize

---

Jean Fontaine

Supervisors: Prof. François Chaumont &

Estelle Teirlinckx

Thesis jury: Prof. Frédéric Clotman & Dr.

Alice Berhin

LIBST

LOUVAIN INSTITUTE OF BIOMOLECULAR SCIENCE AND TECHNOLOGY

Acknowledgments

First of all, I would like to show my appreciation to my promoter François Chaumont for accepting me as a Master student but also for his advice and corrections. This opportunity gave me confidence and determination for what I want to pursue in life.

I am also extremely grateful to Estelle Teirlinckx, my supervisor who guided me throughout this year; giving me enough space to learn by myself but always being there to help with her knowledge and her vast skills.

Thanks to the whole AQP team, Maxime, Romina, Lei and the master's students for their good mood, help and counsel during the year. Thanks to all of the members of the FYMO lab for always answering my questions with expertise, patience, and dedication. Your willingness to share knowledge and provide assistance is greatly appreciated.

Finally, I would like to thank my girlfriend Logane, my family and my friends for their support during this master thesis as well as my studies.

List of abbreviations

2,4D	2,4-Dichlorophenoxyacetic
2YT	2x yeast extract and tryptone
A	Alanine
ABA	Abscisic acid
AQP	Aquaporin
ATAF	Arabidopsis transcription activator factor
BMS	Black Mexican Sweet
BSA	Bovine serum albumine
CaMV	Cauliflower mosaic virus
ChIP-seq	Chromatin immunoprecipitation sequencing
CUC	Cup-shaped cotyledon
D	Aspartic acid
DBD	DNA bindng domain
DAP-seq	DNA affinity purification sequencing
E	Glutamic acid
EMSA	Electrophoretic mobility shift assay
eQTL	Expression quantitative trait loci
FAO	Food and Agriculture Organization
G	Glycine
GFP	Green fluorescent protein
H	Histidine
K	Lysine
L	Leucine
LB	Lysogeny broth
M	Methionine

MS	Murashige et Skoog
MYB	Myeloblastosis
N	Asparagin
NAM	No apical meristem
NIP	Nodulin26-like intrisic protein
NLS	Nuclear localization signal
NTL	NTM1-like
ORF	Open reading frame
PCR	Polymerase chain reaction
PIP	Plasma membrane intrinsic protein
Q	Glutamine
R	Arginine
SELEX	Systematic evolution of ligands by exponential enrichment
SIP	Small basic intrinsic protein
T	Threonine
TF	Transcription factor
TIP	Tonoplast intrinsic protein
TM	Transmembrane
TRR	Transcription regulatory region
TSS	Transcription start site
W	Tryptophan
XIP	X intrinsic protein
Y	Tyrosine
Zm	*Zea mays*

List of Figures

List of Tables

Table of contents

1. Introduction

Maize, also known as corn (*Zea mays* L.), has had an increasingly important role in the global agri-food system since it was domesticated approximately 9,000 years ago. Technological advancements, improvements in yield, and expansion of agricultural areas have contributed to a surge in global maize production in recent decades, driven by growing demand. The Food and Agriculture Organization (FAO) of the United Nations estimates that on average between 1987 and 1991, 462 million tons of maize were produced globally each year placing it fifth on a most globally produced crops and livestock ranking while 1,155 billion tons were produced on average between 2017 and 2021 placing it second only to the sugar cane. This versatile crop is primarily used as animal feed globally, but it is also significant as a food crop, particularly in sub-Saharan Africa and Latin America, in addition to non-food applications (Erenstein *et al*., 2022; *FAOSTAT*, 2021). Furthermore, climate change is set to increase the frequency of biotic stresses such as diseases and insect-pests as well as abiotic stresses (e.g. heat, drought, waterlogging) in an unequal manner affecting particularly low-income households in low- and middle-income countries in sub-Saharan Africa, South Asia and Central America (IPCC, 2023). When confronted to those abiotic stress factors, maize develops several responses in a complex and dynamic manner at multiple levels: morphological, physiological, phytochemical and biochemical (Salika & Riffat, 2021). Understanding the molecular and genetic mechanisms of maize in stress conditions such as drought is important in order to have a complete picture and design strategies to improve crop productivity facing the current climate change crisis (Casaretto *et al*., 2016).

1.1. Aquaporins

Water availability is an important issue when it comes to plant abiotic stresses. Three types of water transport exist in plant tissues: the apoplastic path goes through the cell wall, the symplastic path uses the plasmodesmata and the transcellular path goes inside the cells across the plasma membrane (Steudle & Peterson, 1998). The transcellular path is mainly controlled by membrane-bound water channels called aquaporins (AQPs)

(Chaumont & Tyerman, 2014). These 21 to 34 kDa proteins possess 43 homologs in maize (Capuano, 2023; Chaumont & Tyerman, 2014; Laurent, Maistriaux, Chaumont, unpublished data; Su *et al*., 2022).

As they control the membrane osmotic permeability, AQPs have a sizable impact on numerous physiological processes such as root water transport, plant growth and development (Chaumont & Tyerman, 2014; Gomes *et al*., 2009; Yaneff *et al*., 2015). In addition, AQPs facilitate the diffusion of other molecules aside from water. Indeed, other small solutes such as urea, CO_2, H_2O_2, ammonia, metalloids and, as recently reported, ions, O_2, and Al-Malate can move through AQPs, which relates to their multiple physiological capabilities (Bienert & Chaumont, 2014; Byrt *et al*., 2017; Chaumont & Tyerman, 2014; Di Giorgio *et al*., 2016; Fox *et al*., 2017; Gerbeau *et al*., 1999; Gomes *et al*., 2009; Uehlein *et al*., 2017; Y. Wang *et al*., 2017; Zwiazek *et al*., 2017).

Vascular plant AQPs fall into five different subfamilies depending on their sequence similarity: the plasma membrane intrinsic proteins (PIPs), the tonoplast intrinsic proteins (TIPs), the Nodulin26-like intrinsic proteins (NIPs), initially identified in the symbiosomes of legumes but also found in the plasma membrane and endoplasmic reticulum, the small basic intrinsic proteins (SIPs) localized in the endoplasmic reticulum, and the X intrinsic proteins (XIPs) present in the plasma membrane (Bienert *et al*., 2011; Chaumont *et al*., 2001; Chaumont & Tyerman, 2014; Danielson & Johanson, 2008; Ishikawa *et al*., 2005; Johanson *et al*., 2001; Kammerloher *et al*., 1994). The *Z. mays* PIP subfamily members are usually located in the plasma membrane and subdivided in two groups: PIP1 and PIP2 (Gomes *et al*., 2009; Kammerloher *et al*., 1994). ZmPIPs have different expression patterns depending on their location and their development stage as illustrated in Figure 1, which shows high expression of ZmPIPs in roots (Fox *et al*., 2017; Hachez *et al*., 2012). As they are involved in water movement, ZmPIPs play important roles when it comes to response to stress as reviewed by Afzal *et al*. (2016).

PIPs are highly regulated at different levels including gene transcription, protein abundance, trafficking in the secretory pathway and opening/closure (gating), providing plants with the means to rapidly and reversibly modify the cell water permeability

(Chaumont and Tyerman, 2014). Strangely, few data are available regarding the mechanisms regulating their expression at RNA levels and the involved transcription factors (TFs).

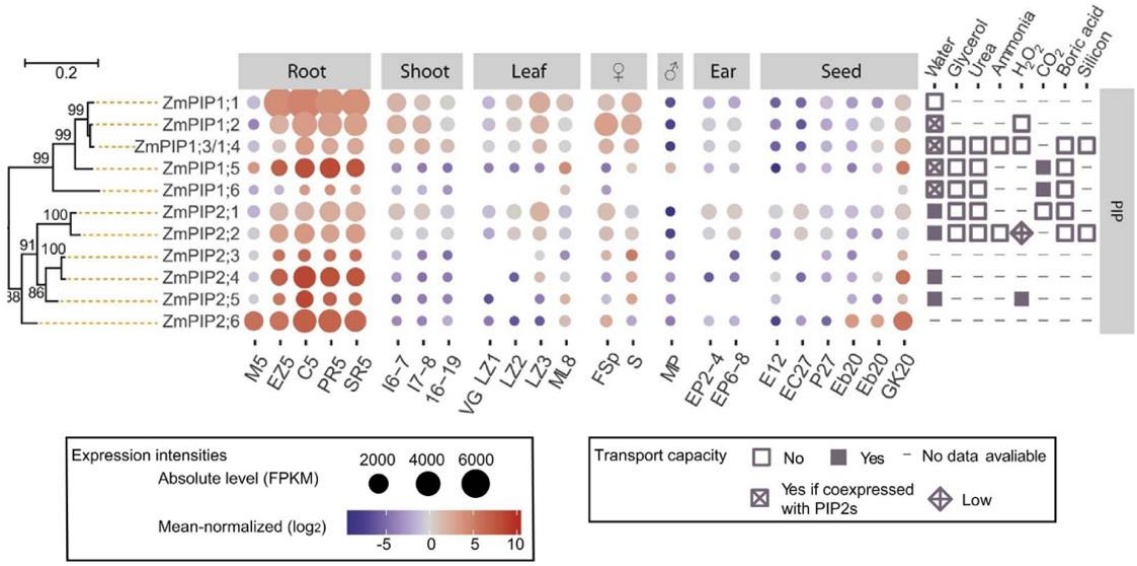

Figure 1: Summary of ZmPIP mRNA gene expression. Absolute expression intensities correspond to the circle size, the circle color indicates the relative expression of the gene normalized for the specific tissue. The distance tree was built using the neighbor-joining method using MEGA7 software. Bootstrap (3000 iterations) are expressed as percentages above the branches. The organs are root meristem, elongation zone, cortex at day 5, and primary root at day 5 (M5, E5, C5, and PR5), secondary root at day 7–8 (SR7-8), internode at day 6–7 (I6-7) and at day 7–8 (I7-8), vegetative meristem at day 16–19 (VM16-19), leaf zone 1 (symmetrical) (LZ1), 2 (stomatal) (LZ2), 3 (growth) (LZ3), mature leaf at day 8 (ML8), female spikelets (FSp), silk (S), mature pollen (MP), ear primordium 2–4 mm and 6–8 mm (EP2-4 and EP6-8), endosperm at 12 DAP (E12), endosperm crown and pericarp/aleurone at 27 DAP (EC27 & P27), embryo at 20 and 38 DAP (Eb20 & Eb38) and germination kernel at 2 DAJ (GK2). It also summarizes the different substrate specificities that have been studied so far (Modified.from Fox et al., 2017).

1.2. NAC transcription factors

1.2.1. Plant transcriptions factors

Plants exhibit highly similar fundamental mechanisms to other eukaryotic kingdoms. However, as plants are sessile organisms, they evolved distinct molecular processes in order to adapt to the ever-changing environment, which will often be through the use of specific gene regulatory cascades (Hao *et al*., 2010). Gene expression is generally

modulated by the combined action of multiple elements close to the gene itself also called *cis*-regulatory elements. The core promoter is the center of this organization as it is located upstream of the transcription start site (TSS) and its role is to assure the correct binding and positioning of the RNA polymerase II (in eukaryotes) (Danino *et al*., 2015; Juven-Gershon *et al*., 2008; Lenhard *et al*., 2012; Spitz & Furlong, 2012). *Cis*-regulatory elements contain sequences that function as transcription factor (TF) binding sites. TFs are proteins that will recognize these binding sites through a small 6-12 bp sequences called binding motifs (Spitz & Furlong, 2012), increasing or decreasing gene expression level through multiple mechanisms. Other *cis*-regulatory modules may be located further from the TSS namely transcriptional enhancers, silencers, insulators and tethering elements (Spitz & Furlong, 2012). For example, enhancers are often placed thousands of base pairs up- or downstream of their regulated gene but have an important influence on its transcription (Gonzalez, 2015; Weber *et al*., 2016), by primarily recruiting pioneer TFs, which will engage other cofactors such as histone acetyltransferase and chromatin remodelers whose role is to physically clear a path for other TFs by making the promoter more accessible and thus increasing gene transcription (Iwafuchi-Doi & Zaret, 2014; Weber *et al*., 2016).

Concerning their structure, TFs all contain a DNA Binding Domain (DBD), which recognizes the binding motif. Many types of DBDs exist and each can be made of alpha helices, beta sheets as well as disordered regions and some even use cations (Gonzalez, 2015; Pabo & Sauer, 1992). Furthermore, TFs need a nuclear localization signal (NLS) that allows them to be recognized and translocated into the nucleus after being synthesized in the cytosol. The NLS can vary from protein to protein, classical NLSs being characterized by four to ten amino acid residues rich in positively charged residues such as arginine (R) and lysine (K). There are also non-classical NLSs that can, for example, be 20 to 30 amino acid residues long (Gonzalez, 2015; Jans *et al*., 2000; Kalderon *et al*., 1984; J. Lu *et al*., 2021). In addition, TFs also contain transcription activation and/or repressor domains but they lack motifs as easily recognizable as DBDs (Hao *et al*., 2010). Finally TFs may also contain domains that enable them to form homo-

or heterodimers and complexes with other TFs (Pabo & Sauer, 1992; Spitz & Furlong, 2012).

1.2.2. The NAC Family

Plants have several specific TFs families, including the AP2/ERF, WRKY, TCP and NAC families (Gonzalez, 2015). The NAC acronym gets its name from three reported proteins that contain a highly conserved domain in their N-terminal region (the NAC domain): NAM (No Apical Meristem), ATAF1/2 (*Arabidopsis thaliana* Transcription Activator Factor 1/2) and CUC2 (Cup-shaped Cotyledon 2) (Aida *et al*., 1997). NAC TFs have been studied in many plant species and have been determined to influence various plant processes: development, maturity, immunity, biotic and abiotic stress responses (Kim *et al*., 2016; G.-S. Liu *et al*., 2022; Podzimska-Sroka *et al*., 2015; G. Wang *et al*., 2016; Yuan *et al*., 2019).

1.2.2.1. Structure

NAC proteins contain a highly conserved domain called the NAC domain, which is located at the N-terminus, and a transcription regulatory region (TRR) at the C-terminus. The NAC domain is usually 150 amino acid long and is described as having five conserved subdomains (named A to E), some NAC members possess two consecutive NAC domains (Olsen *et al*., 2005). Its 3D structure is conserved between the different NAC proteins. *Arabidopsis thaliana* NAC019 (ANA019) NAC domain was the first to be determined through X-ray crystallography (Ernst *et al*., 2004) and was described as "a twisted antiparallel β-sheet sandwiched between two helices". Indeed, this fold is a seven-stranded antiparallel twisted β-sheet (named β1 to β7) flanked by an α-helical element on either side of the strand and is the default NAC domain structure of a typical NAC protein. The β1-3, β3-6 and β6-7 strands are respectively contained in the subdomains C, D and E.

In 2011, Chen *et al*. also reported a crystal structure of the rice stress-responsive NAC1 (SNAC1) which is strikingly similar to ANAC019 one as observed in Figure 2, which displays a superposition of both NAC domains.

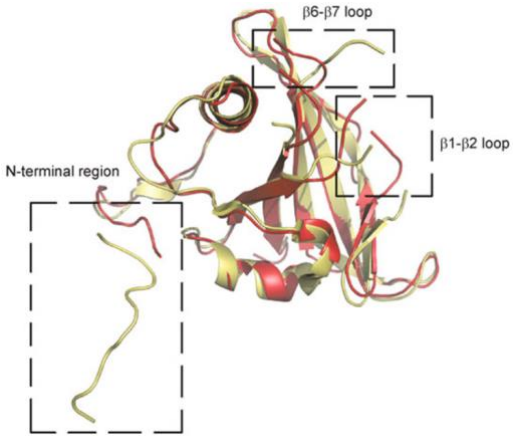

Figure 2: Superposition of SNAC1 NAC domain (red ribbon) and ANAC019 NAC domain (yellow ribbon) (Q. Chen et al., 2011).

A few differences can be observed, notably in the N-terminal region and the β1-β2 and β6-β7 loops, which is hypothesized to be related to their respective biological functions (Q. Chen *et al*., 2011). Concerning the DNA binding properties, V119-S183 (β4-6; subdomain D-E), K123 and K126 (β4-5; subdomain D) and K79, R85 and R88 (β1-2; subdomain C) are critical for the protein with R88 found to be conserved so far in all NAC proteins (Puranik *et al*., 2012). The presence of K79 and R85 being more variable is proposed to be a potential explanation for the varying DNA binding intensity between NACs (Jensen *et al*., 2010). Conversely, the β4-5 region of the NAC domain contains a sequence of multiple hydrophobic amino acids (LVFY), which could indicate the presence of a transcriptional repressor domain (Hao *et al*., 2010; Welner *et al*., 2016). It is within the subdomain D that the NLS can be found (Tran *et al*., 2009), and the subdomain A plays a role in dimer formation through the L14–T23 and E26–Y31 residues (Ernst *et al*., 2004; Jensen *et al*., 2010; Olsen *et al*., 2005; Puranik *et al*., 2012). SNAC1 and ANAC019 are functional homodimers using a combination of hydrophobic interaction, hydrogen bond, salt bridge and Van der Waals interaction in order to dimerize (Q. Chen *et al*., 2011; Olsen *et al*., 2005). The NAC domain is also linked to protein binding activities such as stress tolerance (Olsen *et al*., 2005; Singh *et al*., 2021; Tran *et al*., 2007; Yamaguchi *et al*., 2010). Even more recently, a third NAC domain crystal structure of a NAC, ORE1 (*A. thaliana* NAC092), has been obtained (Chun *et al*., 2022).

It is also very similar in its structure to the two other ones and presents a clear dimeric crystal structure (Figure 2).

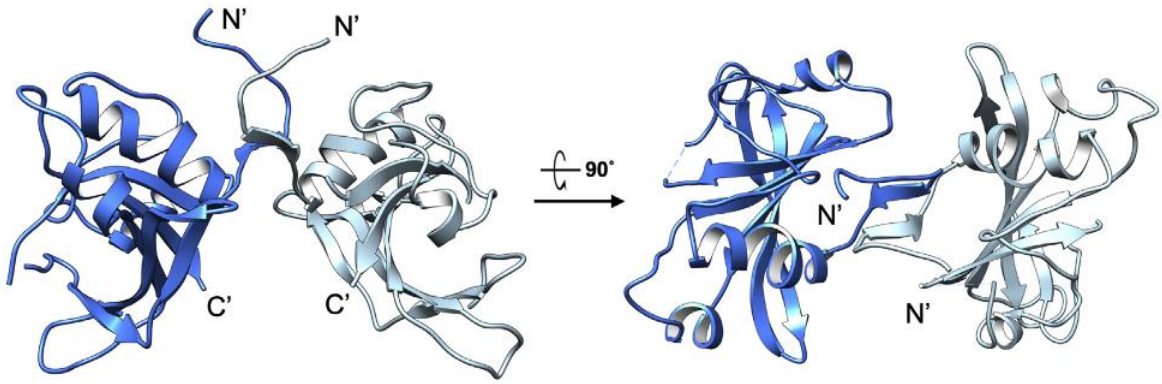

Figure 3: Crystal structure of the ORE1–NAC domain dimer not bound to the DNA represented in the ribbon diagram. One monomer is shown in blue and the other in pale blue (Chun et al., 2022).

Concerning the C-terminal TRR, it contains multiple repeating motifs of S–T, P–Q or acidic residues which, depending on the subgroup of each NAC subfamily, remain conserved for their respective subgroup, indicating that it is linked to each subgroup function (Puranik *et al*., 2012; Shen *et al*., 2009). This region is thus characterized as having low complexity that causes three-dimensional structures to be unstable but it also confers protein-binding abilities as well (Kleinow *et al*., 2009). An α-helical transmembrane motif (TM) has been observed in some particular NAC proteins named NTL (NTM1-Like, NTM1 being a NAC possessing that TM), which anchors the protein to the plasma membrane or endoplasmic reticulum (Diao *et al*., 2020; Puranik *et al*., 2012; P. J. Seo *et al*., 2008). Other multiple variations can occur in NAC proteins. The N-terminal part can be extended before the NAC domain, or the TRR and NAC domain can see their positions inverted with the former in the N-terminus and the latter in the C-terminus (Puranik *et al*., 2012).

1.2.2.2. DNA Binding Domain

The β3 strand of the NAC domain core β-sheet has a positive charge, and seems to protrude from the domain into the DNA groove as a possible recognition and binding mode for the protein (Ernst *et al*., 2004; Welner *et al*., 2016; Zhu *et al*., 2014). Indeed,

this β3 strand contains residues forming the recognition motif WKATGTDK similar to the characteristic WRKYGQK motif of WRKY TFs, which is linked to the DNA-binding abilities of this family (Jensen *et al*., 2010; Welner *et al*., 2016; Yamasaki *et al*., 2012). It also contains a glycine residue (G99 in ANAC019) which induces a curvature in the strand that follows the DNA groove (Welner *et al*., 2016). Not all positive amino acid residues seem to interact directly with the DNA strand, some may be involved with the DNA recognition. Furthermore, H141 residue in ORE1 has the crucial task to accommodate the multiple positive charges surrounding it, in order to conserve the general structure of the DBD.

As ORE1 functions as a homodimer, it requires a particular consensus sequence (TTNCGTG) ordered in a palindromic manner with a 5-bp linker between in order to bind to the DNA strand (total 19 bp) (Figure 4) (Chun *et al*., 2022; Olsen *et al*., 2005). Interestingly, ORE1 still binds to the DNA as the linker length is shortened by 1 bp or lengthened by 3 bp while gradually decreasing in binding strength, which indicates some flexibility in the dimer with a limited angle of closure and a more flexible opening angle (Chun *et al*., 2022). This dimer angle can vary from about 120° in the open conformation to about 100° in the closed formation. While in the absence of DNA, the open conformation seems to be preferred, and the closed one is predominant when binding occurs.

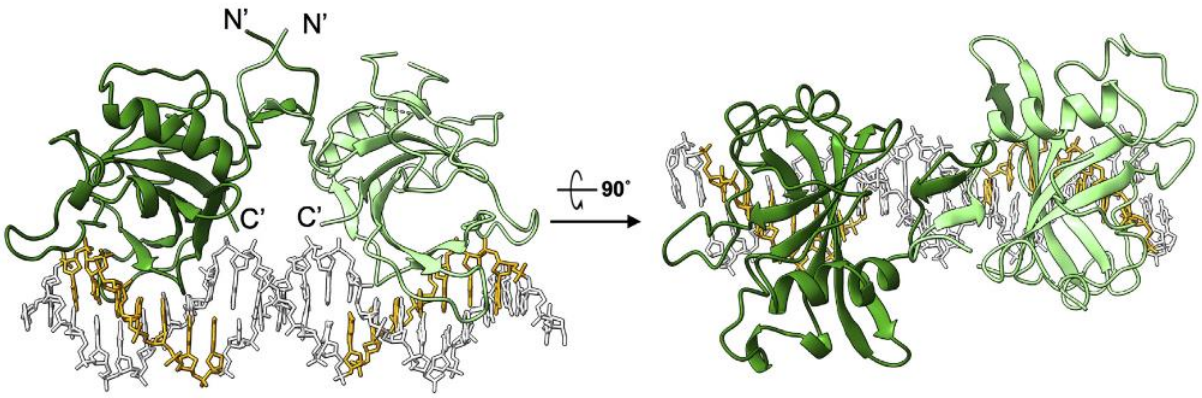

Figure 4: Crystal structure of the ORE1–NAC domain-DNA complex. One monomer is shown in green and the other in pale green. DNA is presented in white, and the consensus sequence is colored in orange (Chun et al., 2022)

As said previously, NAC TFs possess resemblance with the WRKY TF family. The WRKY TFs constitute one of the largest TF families in plant (Bakshi & Oelmüller, 2014). They have a β strand, analogous to the NACs β3 strand, which bears the family defining WRKY DBD (WRKYGQK) and a glycine, which fulfills the same function as the one from NAC TFs (Welner *et al*., 2012). The mammalian glial cell (GCM) TF family is also often compared to NAC and WRKY TFs (Welner *et al*., 2012). They have a less resembling recognition motif than the other two families (MRNTNNHN) but their DNA binding modes are very similar with a core β sheet. While WRKY and GCM share a binding motif, which utilizes a Zn cation, NAC does not. In addition, NAC TFs are the only ones of the three to show dimeric conformations (de Beer *et al*., 2014; Welner *et al*., 2012, 2016).

1.2.2.3. Transcriptional regulation of NAC TFs

As transcription is the first step for protein production, it is also the first step where regulation can occur. Recognition sequences from various TFs are present in *NAC* promoter regions but not much is known about their regulatory mechanism (Nakashima *et al*., 2012; Puranik *et al*., 2012). Additionally, some of them have NAC binding sites in their promoter region, which indicates the involvement of NACs upstream in the NAC regulatory network with possible autoregulation and cross-regulatory mechanisms (Kim *et al*., 2014, 2016). NAC TFs possessing stress-related abilities (called stress-responsive NAC or SNAC) are the most studied, especially their regulatory pathways as it is necessary to understand plant stress resistance (Diao *et al*., 2020; Jensen *et al*., 2010). SNACs may also have their expression regulated by *cis*-acting elements situated in the promoter region such as ABA-responsive elements, low-temperature responsive elements, myeloblastosis (MYB) binding sites as well as W-Box, jasmonic acid responsive element and salicylic acid responsive element (Nakashima *et al*., 2012; Puranik *et al*., 2012). All those elements are linked to stress response; for example, ABA is a prominent plant hormone that acts in case of abiotic stress (Diao *et al*., 2020). Besides the transcription, *NAC* gene expression can be regulated by micro-RNA (miRNA) but also alternative splicing and *trans*-splicing (Mathew & Agarwal, 2018; Puranik *et al*.,

2012). For instance, the *Zm-miR164* family in maize targets *ZmNAC* genes during internode elongation (Yang *et al*., 2022). As for *post*-translational regulation, multiple examples of protein degradation mediated by ubiquitin (W. Guo *et al*., 2015), dimerization (Jeong *et al*., 2009) and interaction with other non-NAC proteins exist (Greve *et al*., 2003; Puranik *et al*., 2012).

1.2.2.4. Phylogeny of NAC TFs

As the central β-sheet DBD shares similarity with the WRKY and GCM families along with their recognition motif, it is hypothesized that they share a common origin. WRKYs are present in primitive eukaryotes, while NACs and GCMs are specific to plant and metazoan, respectively. This information presents WRKYs as ancestors of NACs and GCMs (Mathew & Agarwal, 2018). In the plant kingdom, NAC TFs are ubiquitous in land plants and evidence suggests that they emerged 725–1200 million years ago when the streptophytic green algae has moved from an aquatic to a terrestrial environment (Mathew & Agarwal, 2018).

In maize, 148 nonredundant *NAC* genes (*ZmNAC1-ZmNAC148*) were identified thanks to their NAC domains by Peng *et al*. (2015), through a genome-wide survey using Blast search tools. These NAC members were divided into 12 groups (named A to L) based on phylogeny. The authors generated an unrooted joined phylogenetic tree (Figure 5) and used well-characterized non-maize NAC TFs in order to have a better understanding of the function of each group. For example, the previously mentioned ANAC019 and SNAC1 are found in the stress-related group as expected. Group A contains 22 proteins, which are not published as NAC indicating a maize-specific group (Peng *et al*., 2015). Wang *et al*. (2020) also performed a transcriptome analysis on a drought-resistant inbred maize line under PEG stress and rewatering treatment and found 87 out of 147 *ZmNAC* genes responsive to drought stress and categorized them into 15 groups (G. Wang *et al*., 2020).

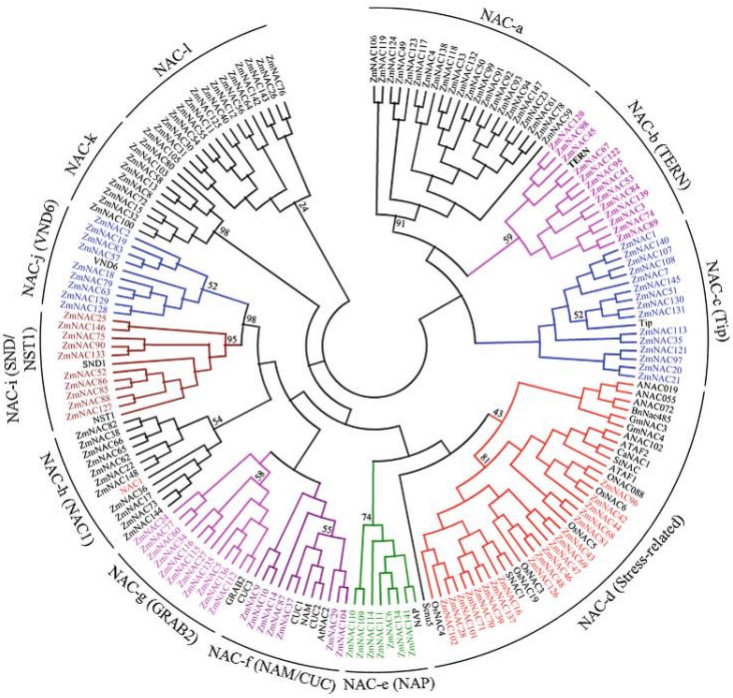

Figure 5: Joined phylogenetic tree of NAC proteins from maize and other plant species. The full-length amino acid sequences of 148 maize and 32 other species NAC genes were aligned by Clustal X 1.83 and the phylogenetic tree was constructed using MEGA 4.0 by the N–J method with 1000 bootstrap replicates. Each NAC subfamily is indicated in a specific color (Peng et al., 2015).

1.2.2.5. NAC TFs play various roles in the maize cell

NAC TFs factors are well studied for their stress response functions, but they serve other purposes as well. For example, a recent study by Yuan *et al*., (2023) showed that ZmNAC132 regulates leaf senescence and male fertility. During leaf senescence, nutrients are remobilized from the leaves to other organs mainly for seeds formation. It is a crucial step for the plant development and fitness with the major nitrogen source coming from the chlorophyl degradation (Lim *et al*., 2007). In this study, 15 *NAC* genes were identified via transcriptome analysis during senescence and *ZmNAC132* transcription changed the most. This gene seems to directly or indirectly activate *ZmNYE1* and *ZmNYE2* expression, which both are major chlorophyl catabolic genes. Furthermore, it also directly activated *ZmEXPB1*, an expansin-encoding gene associated with sexual reproduction and regulating the expression of related genes (Yuan *et al*., 2023). Another study by Zhang *et al*. (2019) studied the way ZmNAC128 and ZmNAC130 regulate accumulation of starch and protein in maize seeds, a process requiring a tight coordination

of specific gene expression. Zein is a cereal seed storage protein and serves as a nitrogen sink for the germinating seedling (Z. Zhang *et al*., 2015). *Bt2* and *16-kD γ-zein*, two zein-linked genes share a common DNA binding site forZmNAC128 and ZmNAC130. This binding site is also found in other genes linked to starch synthesis (*Zpu1*, *GBSS1*, *Sh2*, *SS5*) , which is reduced in *ZmNAC128* and *ZmNAC130* knockout lines (Z. Zhang *et al*., 2019). ZmNAC41 and ZmNAC100 TFs also respond to biotic stresses and are induced after necrotrophic colonization of maize leaves by the hemibiotrophic ascomycete fungus *Colletotrichum graminicola* (Voitsik *et al*., 2013). In fact, multiple binding sites from TFs known to be associated with the plant defense network are located in several maize *NAC* promoters (Bian *et al*., 2020; Voitsik *et al*., 2013).

As said previously, NACs are especially investigated for their abiotic stress-related response as salinity, cold, high temperatures, and mineral toxicity are major causes of reduced crop yields reduction worldwide (Kimotho *et al*., 2019). *ZmSNAC1* is strongly induced by low temperature, high-salinity, drought stress, and ABA treatments with its overexpression leading to an enhanced resistance to dehydration for the plant compared to wild-type seedlings (M. Lu *et al*., 2012). Four *NAC* genes, namely *ZmNAC18*, *ZmNAC51*, *ZmNAC145*, and *ZmNAC72*, were up-regulated in drought-tolerant maize and down-regulated in susceptible maize (Shiriga *et al*., 2014), and seven *ZmNTLs* were highly expressed in the roots and down-regulated in the leaves while subjected to a H_2O_2 and/or ABA treatment. Overexpression of these NTLs resulted in an increased tolerance of H_2O_2 in *A. thaliana* (Kimotho *et al*., 2019; B. Wang *et al*., 2012). Numerous studies in recent years have also continued to bring focus on stress-responsive NAC proteins (Y. Chen *et al*., 2023; H. Liu *et al*., 2023; Luo *et al*., 2022; Xi *et al*., 2022).

1.2.3. ZmNAC24

This TF, which will be hereafter called NAC24, is referred to as NAC-TF 24 in MaizeGDB (accession number: GRMZM2G008374) and by Wang *et al*. (2020), ZmNAC8 (Fan *et al*., 2014), ZmNAC38 (PLAZA database and Shiriga *et al*., 2014) or ZmNAC29 (Peng *et al*., 2015). It possesses a NAC domain, five constitutive subdomains and belongs to the NAM subfamily, which includes NAC TFs involved in shoot apical

meristem and flower development and senescence (Fan *et al*., 2014; Maistriaux, 2021; Peng *et al*., 2015; Shiriga *et al*., 2014; G. Wang *et al*., 2020; Aida *et al*., 1997; Pei *et al*., 2013; Shibuya *et al*., 2014; Souer *et al*., 1996). *NAC24* is located on the lower-end arm of chromosome 2 (position 196582504 – 196584318, B73RefGen_V4), is 1814 bp long with two introns. The protein coding sequence is 1167 bp long and encodes a 388 amino acid residues long protein with a calculated molecular mass of 42.5 kDa (Teirlinckx, 2020; G. Wang *et al*., 2020). NAC24 promoter region contains ABRE, MBS and WRKY binding sites, suggesting that *NAC24* is linked to responses to abiotic stress (Teirlinckx, 2020). In addition, *NAC24* expression was found to be stimulated by drought (after 96h) and repressed after rewatering (Teirlinckx, 2020; G. Wang *et al*., 2020). Figure 6 shows the gene expression level of *NAC24* in different tissues with a notable high expression in the primary roots as well as in the crown roots.

NAC24 came into focus when L. Maistriaux, during her PhD, performed an eQTL study on the variation of maize AQP *ZmPIP2;5* expression in order to localize elements that regulate its expression. As shown in Figure 7, NAC24 came out of this study as a potential regulator of *ZmPIP2;5.* A subsequent reporter assay was carried out and demonstrated that NAC24 *trans*-activates the *ZmPIP2;5* promoter (Maistriaux, 2021). E. Teirlinckx is currently characterizing the relationship between NAC24 and ZmPIP2;5 in the frame of her PhD thesis. A Dual-Luciferase® Reporter assay confirmed the *trans*-activation of the *ZmPIP2;5* and suggested, but did not demonstrate, the direct nature of the binding. An EMSA performed on the *ZmPIP2;5* promoter and NAC24 indicated that the latter binds to the promoter *in vitro*.

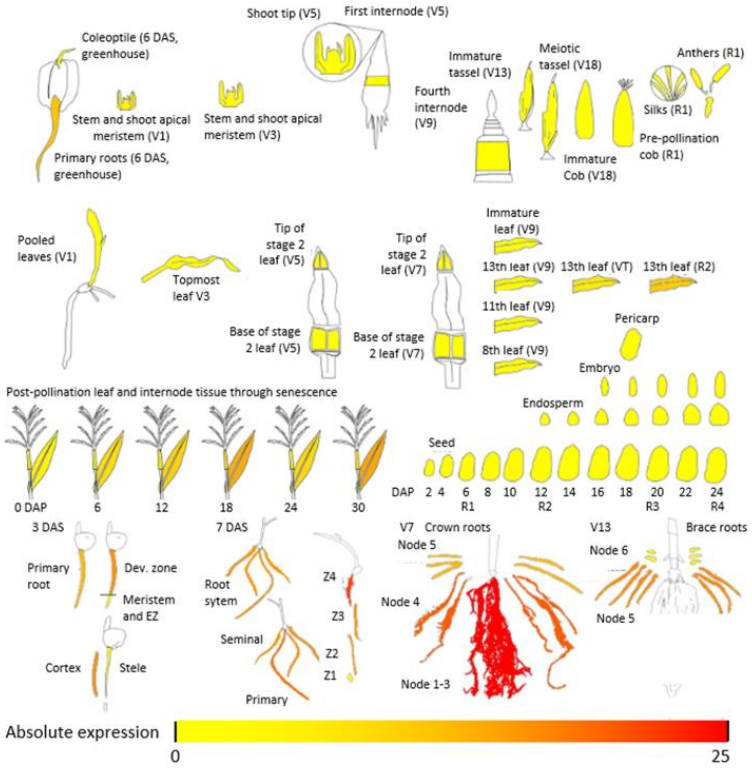

Figure 6: Gene expression in different tissues (represented by pictographs) is represented by color gradient from yellow (low) to red (high), shown for NAC24*. Maize development and codified developmental stages (and the cognate nomenclature) are shown in B, DAS stands for day(s) after sowing and DAP stands for day(s) after pollination. Z stands for zone. Data come from atlas from Hoopes et al., (2019) and Stelpflug et al., (2016). Adapted from original figures from the eFP browser by L. Maistriaux (Winter et al., 2007).*

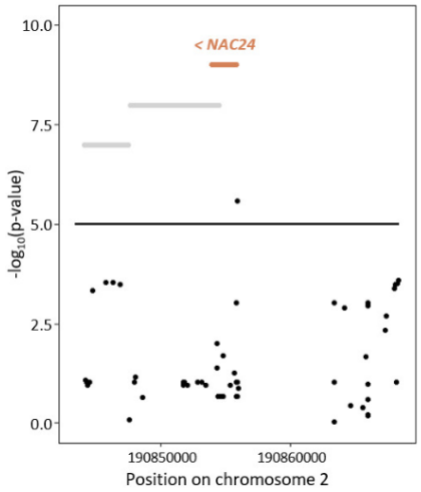

Figure 7: A Manhattan plot of a ZmPIP2;5 *distant eQTL. It is composed of a sole significant SNP (S2-190855919). Its range includes three genes. The* NAC24 *gene is shown in orange. The two other genes are shown in gray. They are described, from left*

to right, as encoding a lipid-binding protein (GRMZM2G305864) and a myosin heavy chain-related protein (GRMZM2G007885) in the PLAZA database (Van Bel et al., 2018).

1.3. Techniques for studying TFs

1.3.1. *In vivo* functional studies

Techniques that study *in vivo* capabilities of TFs usually resemble the ones used to characterize any other gene (Gonzalez, 2015). One of the simplest methods used is to express the TF of interest under the control of a strong promoter. This can be done either in its original organism (homologous expression), or in another organism (heterologous expression), which is generally the case when the species is more difficult to be transformed. The *35S* promoter (*p35S*) from the plant pathogen Cauliflower Mosaic Virus (CaMV) is one of the most used regulatory components (Amack & Antunes, 2020; Gonzalez, 2015). However, *p35S* is active in most tissues (driving an ectopic expression) where the *TF* gene may be repressed or not expressed (Gonzalez, 2015; Katagiri & Chua, 1992). Overexpression as well as ectopic expression can both bring information about the TF functions, but have downsides. Firstly, ectopic expression does not completely correlate with endogenous expression. Secondly, overexpression can interfere with other mechanisms/equilibriums as TF genes are usually low expression levels (Cao *et al*., 2021; M. Chen *et al*., 2007; Gonzalez, 2015; Zheng *et al*., 2009).

This approach does have multiple variations. Using another promoter, known to work in a specific place or during a specific development stage, can give useful information. The use of an inducible promoter is an alternative option to enable the experimenter to launch the expression when desired. This allows the understanding of the variations that happen soon after the TF is expressed. Expression of a mutated form of the TF with, for instance, a disabled DBD or protein-protein interaction domain will cause disruptions in the studied cells that can differ from the simple overexpression (Gerasimavicius *et al*., 2022). Gain-of-function mutants will work in a similar but opposite way. For example, a supposed DBD can be enhanced by increasing the number of positive amino acid residues, thus

binding more targets, which can disrupt the cellular machinery (Gerasimavicius *et al*., 2022).

Disabling the TF is also extremely useful as it shows the impact its absence has on the studied system. The gene coding for the studied TF can be knocked out by selecting cell lines where it has been silenced using T-DNAs or the CRISPR/Cas9-mediated genome editing system (B. Wang *et al*., 2020).

1.3.2. *In vitro* protein-DNA interaction studies

1.3.2.1. Electrophoretic Mobility Shift Assay (EMSA)

Originally described by Fried & Crothers (1981) and Garner & Revzin (1981), EMSA is based on the principle that the electrophoretic mobility of a protein-nucleic acid complex will be slower than the free nucleic acid in a nondenaturing polyacrylamide gel (Gonzalez, 2015; Hellman & Fried, 2007). It is a quick, simple, sensitive and quantitative method to detect protein-nucleic acid interaction (Carey, 1991; Fried & Crothers, 1981; Fried, 1989; Fried & Garner, 1998; Garner & Revzin, 1986; Gonzalez, 2015; Hellman & Fried, 2007; Lane *et al*., 1992). In the context of TF characterization, oligonucleotide or DNA fragments, usually ranging from 30 bp to 200 bp, are used and labeled radioactively or with fluorescent dyes (Gonzalez, 2015; Steiner & Pfannschmidt, 2009; Viola & Gonzalez, 2011). The TF used in the assay is purified which is useful to test its ability to bind DNA and test different DBD mutations (Gonzalez, 2015). As previously mentioned, EMSA is also quantitative and is used for equilibrium and kinetic studies (Gerstle & Fried, 1993). A combination with a Western blot analysis or mass spectrometry is also possible (Hellman & Fried, 2007). This method does present some limitations: the gel matrix is quite different from a solution and the free DNA or protein-DNA complexes can diffuse within the gel, which can make accurate analysis complicated (Flores *et al*., 2015; M. Seo *et al*., 2019). In addition, the samples are not at equilibrium when the electrophoresis step begins, which means rapid dissociation can make interactions undetected (Hellman & Fried, 2007).

1.3.2.2. Systematic Evolution of Ligands by Exponential enrichment (SELEX)

SELEX is used to determine the *in vitro* DNA-binding sequence capabilities of TFs including the binding motifs and the specificity of the binding. SELEX uses multiple steps of binding and amplification in order to progressively amplify a specific TF target sequence from a large double-stranded DNA library (Blackwell & Weintraub, 1990; Gonzalez, 2015; Oliphant *et al*., 1989). Indeed, a DNA library compiling every possible 20-30 bp sequence flanked by adaptors, later used in the amplification, is put in contact with the studied TF. The unbound DNA is then separated from the protein-DNA complexes using EMSA, nitrocellulose membrane filtration, affinity surface/tags, crosslinking or antibody-based flow cytometry (Gonzalez, 2015; Gopinath, 2007). The recovered DNA fragments are amplified through polymerase chain reaction (PCR) using primers specific to the adaptors and put again in contact with the TF. This cycle is repeated multiple times (4 – 18) for decreasing any nonspecific binding chances, and the sequencing of the final DNA fragments results in a consensus sequence for the binding motif (Gonzalez, 2015; Gopinath, 2007; Grotewold *et al*., 1994; Huang *et al*., 1993; Nole-Wilson & Krizek, 2000; Tuerk & Gold, 1990). Its main drawbacks are that it is a slow and laborious method, typically taking 4 – 6 weeks to complete 8 – 12 cycles, and it uses large quantities of reagents and target molecules (Berezovski *et al*., 2005; Bowser, 2005; Y. Liu *et al*., 2012; Lou *et al*., 2009; Y. X. Wu & Kwon, 2016).

1.3.2.3. Footprinting assay

Also known as protection assays, the basic principle of footprinting assay is as follows: DNA strands are put in contact with the TF and cleaved with DNAse I after binding. The unbound DNA is unprotected and thus cleaved while the protein-DNA complex creates steric hindrance, and no cleavage occurs (Galas & Schmitz, 1978; Gonzalez, 2015). Typically, the affinity of a TF with its binding site is greater than the DNase I, thus the sites bound to the TFs are being spared from DNase I cleaving (N'soukpoé-Kossi *et al*., 2008; Pellerin *et al*., 1994; Renda *et al*., 2007; Vierstra & Stamatoyannopoulos, 2016).

The conditions of the reaction are adjusted so that only one cleavage happens on average per strand. One of the DNA strand ends is labeled and after a denaturing polyacrylamide gel electrophoresis, a comparison between the unbound DNA and the protein-DNA sample patterns gives information on the regions protected by the bound TF. The bound DNA can then be sequenced. Modifying certain parts of the DNA, which are suspected of being involved in the binding process prior to the reaction is another method that can be used to determine a TF binding motif and the bases with which it interacts (Gonzalez, 2015). This method is often used in cooperation with EMSA as it provides an environment where the binding equilibrium can be reached, but its detection is less sensitive than EMSA, which makes the two methods complementary (Hellman & Fried, 2007).

1.3.2.4. Microarray-based analysis

Protein-binding microarray (PBM) is a more recent method that permits a higher throughput of *in vitro* DNA binding sequence specificity than the previously mentioned techniques. Additionally, PBM also detects TF binding sites that present a lower affinity with the TF but are still functionally significant in transcription regulation, and which might not be detected by other methods (Amendt *et al*., 1999; Bulyk *et al*., 1999, 2001; Gonzalez, 2015; Mukherjee *et al*., 2004; Walter et al., 1994). In microarray-based analysis, a tagged purified TF is incubated on a double-stranded DNA microarray and then washed. A reporter (i.e., an antibody) that has an affinity for the tag emits a signal as it binds to its TF bound to the DNA. This signal is detected and measured (Gonzalez, 2015).

1.3.2.5. DNA Affinity Purification sequencing (DAP-seq)

The fact that both SELEX and PBM function with synthetic oligomers can be a limitation as these DNA fragments lack genomic context. DAP-seq brings a combination of affinity purification of genomic DNA fragment with TFs and next generation sequencing, to obtain a higher throughput analysis generating genome-wide binding site maps as well as a more down-to-earth approach than the previously mentioned methods, due to the use of

genomic DNA versus synthetic DNA (M. Li & Huang, 2022; O'Malley *et al*., 2016). First, a DNA library, containing approximately 200 bp fragments, is prepared by shearing genomic DNA (gDNA), which is then repaired, tailed with adenosines, and ligated with PCR adaptors. Secondly, the TF of interest linked with an affinity tag is produced, usually by *in vitro* expression, and bound to ligand-binding beads. Washing steps help to clear out any leftover cellular components. Thirdly, the purified TFs bound to the beads are brought into contact with the gDNA library, with the relevant gDNA binding to the TF while the rest is washed away. Finally, the bound gDNA is eluted and amplified by PCR where specific sequencing primers will be added to the adaptors for sequencing. After sequencing, a bioinformatic analysis is required, with each reads mapped onto a reference genome where each enriched locus (peak) will be useful in determining TF binding sites and motifs (O'Malley *et al*., 2016). Figure 8 shows an illustration by Bartlett *et al*. (2017) describing the DAP-seq process. The usual DAP-seq protocol uses an *in vitro* HaloTag as affinity tag but the TF bound to a GST tag expressed in *E. coli* is another option that is more cost-effective but time-consuming, especially if several TFs are tested at the same time (Bartlett *et al*., 2017). DAP-seq does retain tissue/cell-line-specific secondary modifications (such as methylation) and features. These can also be erased by amplifying the DNA library before contact with TF in a process called AmpDAP-seq, this will give information on binding sites usually not available to the TF due to secondary DNA modifications when compared with the non-preamplified DAP-seq.

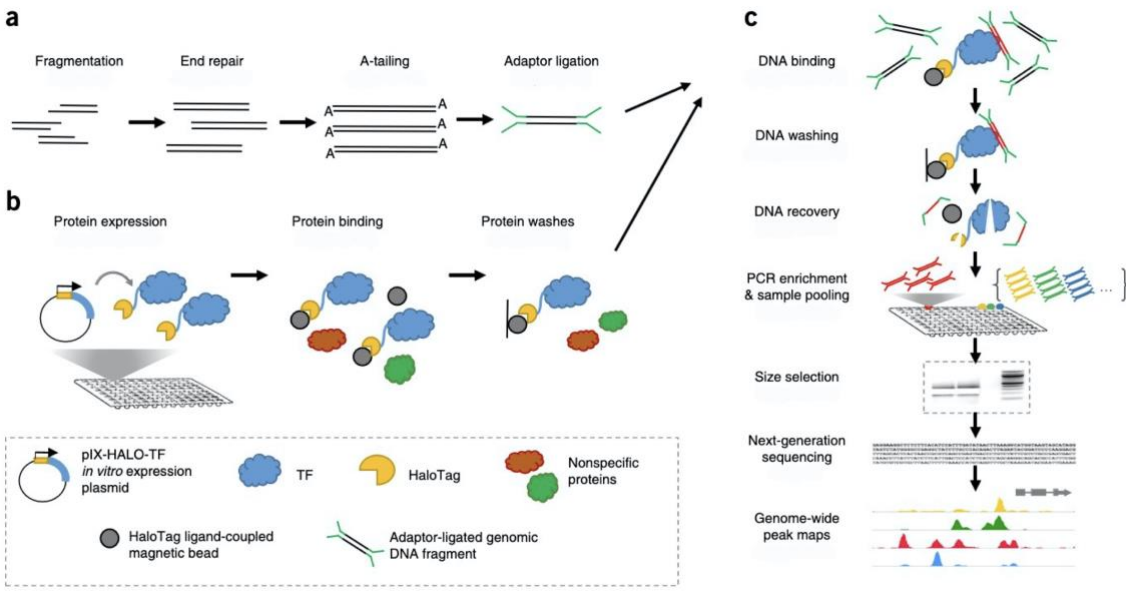

Figure 8: DAP-seq overview using HaloTag. (a) Adaptor-ligated DNA library is prepared: ~200 bp fragments ligated with Illumina-based sequencing adaptors. (b) TF ORF clones fused to the Halo affinity tag are expressed in vitro *and bound to ligand-coupled beads, whereas nonspecific proteins are washed away. (c) HaloTag-TF fusion proteins are incubated with an adaptor-ligated genomic DNA library, and unbound DNA fragments are washed away. Samples are heated to release TF-bound DNA, and the recovered DNA is PCR-amplified to attach indexed sequencing primers. Indexed DNA samples are subsequently combined and size-selected to remove residual adaptor dimers. Purified DNA libraries are sequenced using next generation sequencing, and the resulting genome-wide binding events are analyzed. Peaks shown are maize DAP-seq peaks viewed in the Integrative Genomics Viewer (Bartlett et al., 2017; modified).*

1.3.3. *In vivo* protein-DNA interaction studies

Besides *in vitro* characterization techniques, *in vivo* methods also exist that give information on the impact of the cellular machinery on the TF binding. As high-throughput short read sequencing has been maturing for the past two decades and new emerging techniques using long-read sequencing are developed, the list of available methods is growing every year (Hook & Timp, 2023). This means that it is not possible to delve into all possible techniques, thereby only a few that are more relevant in terms of actual feasibility for a master's thesis will be presented.

1.3.3.1. Chromatin Immunoprecipitation sequencing (ChIP-seq)

Even though the above-mentioned methods provide a substantial amount of information on TF characteristics, they lack the cellular context in which elements such as chromatin accessibility and histone modifications can impact TF binding capacities. The first ChIP protocol was established by Gilmour & Lis (1984, 1985). The first step is to crosslink the DNA-bound proteins by covalently linking DNA with physically interacting proteins. Next, the cells are lysed to extract the gDNA. After extraction, this gDNA is sheared into fragments ready for sequencing. Immunoprecipitation is then performed by introducing an antibody, specific to the protein of interest or a tag fused to it, into the sonicated DNA mixture. This isolates the DNA bound to the protein which is recovered by reverse crosslinking. Analysis is carried out using genome microarrays (ChIP-chip) or high-throughput DNA sequencing in a similar manner to DAP-seq (Gonzalez, 2015; Mardis, 2007; J. Wu *et al*., 2006). Formaldehyde is the most used crosslinking agent due to its quickness, but it can modify the antigen or degrade the protein (Das *et al*., 2004; Gonzalez, 2015). One of the reasons why DAP-seq might sometimes be used over ChIP-seq is the need to express the TF *in vivo* with its tag or to find/develop a suitable specific antibody, which can be quite costly and take more time than *in vitro* transcription translation (Bartlett *et al*., 2017). In addition, ChIP-seq and DAP-seq complement each other quite well, with one providing information to which the other does not have access, and the use of both provides a broader perspective on the whole transcriptional regulation machinery (O'Malley *et al*., 2016).

1.3.3.2. Yeast One-Hybrid assay (Y1H)

Another way to characterize *in vivo* interactions is using the Y1H assay, which is a variation of the yeast-two-hybrid system (Y2H) from Fields & Song (1989) (J. J. Li & Herskowitz, 1993). The principle is the following: two plasmids are transformed into a yeast cell, the first one containing the DNA segment of interest such as a promoter inserted via homologous recombination upstream of a minimal yeast promoter and an associated reporter/selection gene, and the second one containing the TF sequence fused to a yeast activation domain. If the TF recognizes the promoter sequence, it binds to it,

activating the expression of the reporter/selection gene. This method enables the screening of potential million colonies at the same time and is very sensitive (Gonzalez, 2015; Ouwerkerk & Meijer, 2001; Sieweke, 2000). It is important to note that this method leads to the detection of many false positives and only tests direct interactions (Sewell & Fuxman Bass, 2018).

1.3.3.3. Cleavage Under Targets and Release Using Nuclease (CUT&RUN)

CUT&RUN is a more recent alternative to ChIP-seq, designed to reduce the risk of bias from the crosslinking and DNA solubilization steps. Indeed, in this method, TF-specific antibodies fused to a protein A-MNase (pA-MN) are brought into contact with crude nuclei extracts. As the antibodies recognize the TF, the attached pA-MN cleaves the DNA-TF complex from the gDNA strand releasing it into the supernatant in which it is incorporated into a library for sequencing (Skene & Henikoff, 2017a). The method gives a low background because the reaction is performed *in situ,* and is described as more robust, efficient and with better resolution and data quality. Moreover, it can also work for highly insoluble complexes (Skene & Henikoff, 2017a). But limitations remain, the method still depends on the antibody affinity as with ChIP-seq method, which can be problematic,it lacks a crosslinking step (this decreases the efficiency of CUT&RUN), and interactions that are more time-limited could be missed (Skene & Henikoff, 2017b).

1.3.4. Protein-protein interaction studies

The interaction of many TFs is modified by a change in their DNA binding, subcellular localization, and other properties, which can be achieved by transient or permanent physical interaction with other proteins. It is thus important to characterize these interactions in order to have better understanding of the overall process.

1.3.4.1. Yeast Two-Hybrid Assay (Y2H)

Y2H has been the most widely used technique for identifying protein interactions (Fields & Song, 1989; Gonzalez, 2015). Transcription activators are split into two parts, the

DNA-binding domain (BD) and transcriptional activation domain (AD) (Brent & Ptashne, 1985; Gonzalez, 2015; Hope & Struhl, 1986; Keegan *et al*., 1986). These two protein domains do not need to be covalently linked in order to function, and fusing each one to a studied protein is a way to detect an interaction. As these proteins interact together, BD and AD are close to each other and can activate transcription of the reporter gene, thus signaling the interaction between both proteins. The GAL4 transcription activator is often used in yeast cells, where the two domains are each fused to a studied protein along with a NLS used for nuclear trafficking (Fields, 2009; Gonzalez, 2015). This method has been often used for plant proteins (as reviewed by (Lalonde *et al*., 2008; Uhrig, 2006; Y. Zhang *et al*., 2010)(Gonzalez, 2015).

1.3.4.2. Other techniques

Other methods exist for detecting protein-protein interaction, such as (i) *in vivo* expression of the TF of interest fused to an affinity tag followed by chromatography purification and protein analysis (Western blotting, mass spectrometry…) (Gonzalez, 2015), (ii) split reporter protein in which each part of the reporter is fused to one of the proteins of interest and the reconstitution of the reporter protein analyzed, or the fluorescent resonance energy transfer (FRET) method using two fluorophores with overlapping emission/absorption spectra (Gonzalez, 2015). Finally, a recent study by Sönmezer *et al*. (2021) uses the genomic footprinting method to identify TFs binding cooperatively at *cis*-regulatory elements.

2. Objectives

TFs are essential elements of the molecular machinery of gene regulation, and their considerable impact is not fully understood. In the laboratory, we are interested in the involvement of the NAC24 TF in the expression of the *ZmPIP2;5* AQP, discovered in recent years by Laurie Maistriaux and confirmed by Estelle Teirlinckx.

As little is known about NAC24, the aim of this study is to identify its target genes by setting up a DAP-seq protocol in the laboratory as this technique has not yet been performed. Post-sequencing analysis should provide information on NAC24 binding sites and the required binding motifs. This will identify the target genes and enable it to be localized in a gene regulatory network.

The DAP-seq data and ChIP-seq data show a strong synergistic relationship. Therefore, the creation of a stable cell line overexpressing NAC24 for ChIP-seq experiments will be another objective of this work. A choice between two tags will be made in order to obtain the most efficient immunoprecipitation, and a negative control cell line will also be generated. Black Mexican Sweet maize suspension cells are chosen as a suitable expression system in this study, as they could be later studied for physiological tests.

3. Results

3.1. DAP-seq with NAC24

In order to identify NAC24 targets, we choose the DNA affinity purification sequencing approach. DAP-seq requires several steps. First, genomic DNA has to be extracted from maize, sheared, and ligated with sequencing adaptors (see Figure 9.A and B). Secondly, NAC24 is produced *in vitro* fused at its N-terminus to a HaloTag®. A Halo-GFP fusion protein is also synthesized to serve as negative control during the sequence analysis. Then, the produced Halo-NAC24 and Halo-GFP proteins are incubated with magnetic beads (Magne®HaloTag® beads) to which the HaloTag fusion proteins covalently bind, enabling wash steps of the supernatant with minimal protein loss (See Figure 9.C). The gDNA libraries are then put in contact with the bound proteins, and DNA fragments, which are recognized by the TF, are retained while the rest is washed away. The bound DNA is released from the HaloTag fusion protein, amplified with sequencing indexes, and purified. Finally, the recovered samples are sent to Microgen Bioproducts for Illumina sequencing (See Figure 9.D). The protocol from the DAP-seq was adapted from Bartlett *et al*. (2017).

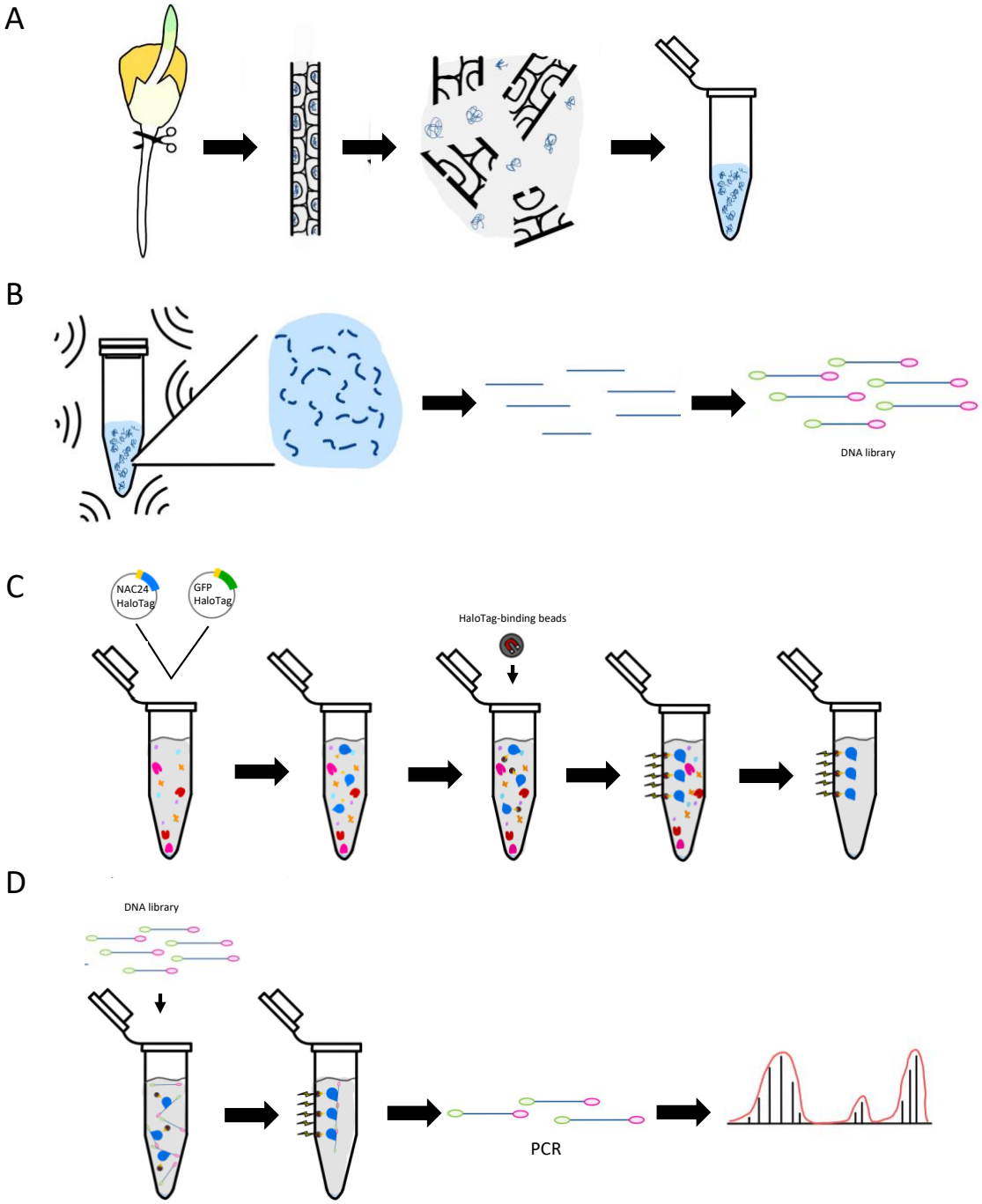

Figure 9: DAP-seq protocol for NAC24 and GFP. (A) Genomic DNA is extracted from maize root cells. (B) It is then sonicated and ligated with sequencing adaptors. (C) HaloTag®- NAC24 or HaloTag®-GFP proteins are synthesized in vitro *and put in contact with HaloTag-binding magnetic beads. (D) gDNA libraries are introduced into the mix and non-bound DNA is washed away. The DNA bound to NAC24 is recovered, amplified via PCR, purified, and sequenced.*

3.1.1. Genomic DNA extraction

As *NAC24* is predominantly expressed in maize primary roots, we extracted gDNA from this tissue, reasoning that NAC24 DNA binding sites are more exposed than in other tissues, where the state of chromatin might make them less accessible. Primary roots were collected and ground 3-day after germination. Genomic DNA was then extractedfrom three roots using Promega Wizard® Genomic DNA purification kit, with yields ranging between 2500 ng to 25000 ng of gDNA recovered per three roots.

3.1.2. Genomic DNA fragmentation

In order to obtain the 200 bp gDNA fragments required for DNA libraries, several methods were tested to obtain optimized and reproducible results. Three sonication machines were available in the lab: the large sonication bath (LB), the small sonication bath (SB), and the sonication probe (SP). Several conditions were tested per machine: for the LB and the SB, 20, 25, 30 and 35 min incubation, and for the SP, 1 x 10 s pulses, and 3 x 10 s pulses, both at 40% amplitude (Figure 10). These tests were not conclusive. The LB and SB were not powerful enough to obtain fragmented gDNA. The SP did not give replicable results probably due to the droplets being expelled while sonicating. However, another researcher in the FYMO group, Dr A. Berhin obtained good gDNA fragmentation using the SB for 20 min and carrying the sonication one or two samples at a time because when the bath was too crowded, it led to unsheared samples. Thus, the SB was used in this way for the following steps. We also tested the amount of gDNA that could be sonicated in the SB at once (Figure 11). DNA seemed to be sheared at the correct size no matter the concentration and 200 bp gDNA fragments were obtained reproducibly, even if there are small variations between each sample. It must be noted that a high initial concentration did not seem to lead to a high signal as can be seen when comparing the 10000 ng samples with the 13500 ng one. This could be explained by the initially calculated DNA being artificially inflated by contaminants such as polysaccharides. It

must also be noted that the unsonicated gDNA has a smear and has a small signal around the 200 bp mark.

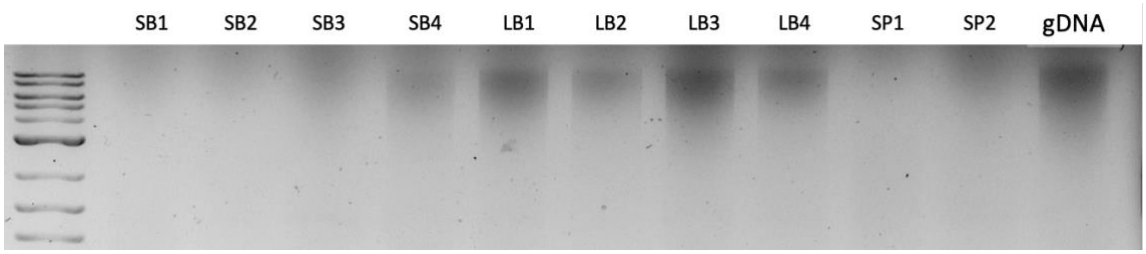

Figure 10: Test for the fragmentation of gDNA for the three available methods: the small sonication bath (SB), the large sonication bath (LB) and the sonication probe (SP) compared to the unfragmented gDNA. For SB1, SB2, SB3 and SB4; samples were left in the bath for 20, 25, 30 and 35 min respectively. The same was done for LB1, LB2, LB3 and LB4. For SP1 and SP2, 1 x 10 s pulses, and 3 x 10 s pulses, both at 40% amplitude were used respectively. The DNA size ladder is on the left.

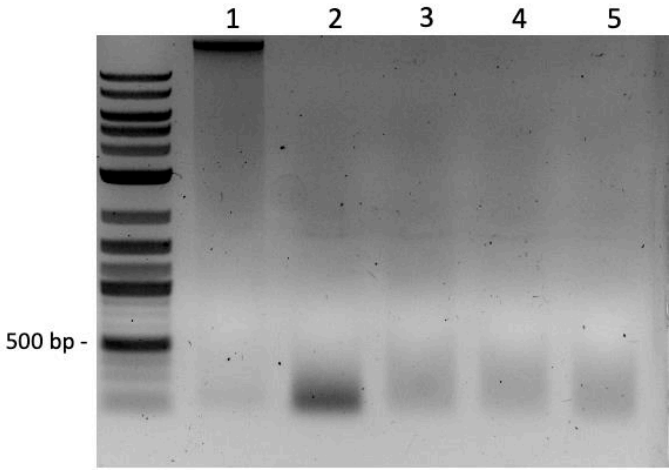

Figure 11: Fragmentation of gDNA to test the amount of gDNA that can be sonicated in the SB. The gDNA is sonicated for 20 min. (1) 8500 ng of unsonicated gDNA, (2) 15000 ng sonicated, (3) 13500 ng sonicated, (4-5) 10000 ng sonicated. Fragments of around 200 bp were obtained for each gDNA concentration. The DNA size ladder is on the left.

3.1.3. gDNA library preparation

The first step of the library preparation was to clean the sonicated gDNA. The original protocol mentioned that the sonicated samples have to be mixed with 3M NaOAc and twice the sample volume of cold 100% ethanol, incubated on ice or at -20°C for 15 min, centrifuged, the supernatant discarded and the pellet washed with 70% (v/v) ethanol

before resuspension in the elution buffer. Due to low DNA recovery rates (20% initial gDNA recovered), some adjustments were made to this protocol. The volume of 100% ethanol was increased from 2 times to 2,5 times the sample volume and was added cold. The incubation was increased to 1 h at -80°C and, if possible, left overnight (o/n) at -20°C after that. The washing was performed with 80% (v/v) ethanol. These changes increased recovery to 35%. Subsequent steps of sample cleaning did not appear to have particularly low recovery rates, being up to 90%, which might indicate that the first cleaning removed contaminants such as carbohydrates that are highly concentrated in roots and can inflate the perceived initial concentration of the sample (Varma *et al*., 2007).

Once this cleaning procedure had been optimized, the following steps required no modifications of the initial protocol. The sheared DNA was repaired in an end-repair reaction, followed by an A-tailing reaction, where a single adenine was added to each side of the repaired ends (using the Klenow fragment that retains the polymerase and 3'→ 5' exonuclease activity, but lacks the 5' → 3' exonuclease activity). Finally, the adaptor ligation step used a Y adaptor, which was ligated through a single thymine that binds to the protruding adenine, this adaptor was subsequently used for the PCR amplification step. A clean-up step was performed between all these steps. To verify that the DNA library had been successfully prepared, PCR amplification was performed on adaptor-ligated DNA and non-adaptor-ligated DNA, using the primers specific to the Y adaptor (Figure 12). Amplification of a band around 300 bp was observed for the DNA library containing only the Y adaptor. The amount of DNA was also checked using the Qubit dsDNA HS Assay Kit (Life Technologies), which uses fluorometry to distinguish double-stranded DNA from other contents such as single-stranded DNA, RNA, protein, and free nucleotides.

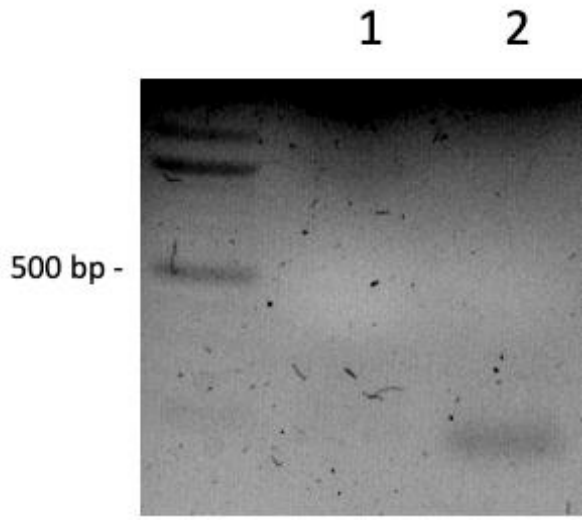

Figure 12: PCR amplification of DNA without Y adaptor (1) and DNA with Y adaptor (2). An amplified DNA band around 300 bp is observed only for the DNA library with Y adaptor. The DNA size ladder is on the left.

3.1.4. HaloTag plasmid construction

The *Halo-NAC24* plasmid used for the DAP-seq was constructed using the Gateway recombination cloning method (Katzen, 2007). The *NAC24* Entry clone plasmid was previously constructed in the laboratory by Maxime Laurent by homologous recombination BP reaction (recombination between attB and attP sites). The Entry clone *NAC24* cassette was then recombined by LR reaction into the destination plasmid, pIX-Halo expression vector, which contains an N-terminal HaloTag (Figure 13) (Los *et al.*, 2008). To serve as negative control, a similar plasmid containing a *GFP* cassette instead of *NAC24* was previously produced by Alice Berhin.

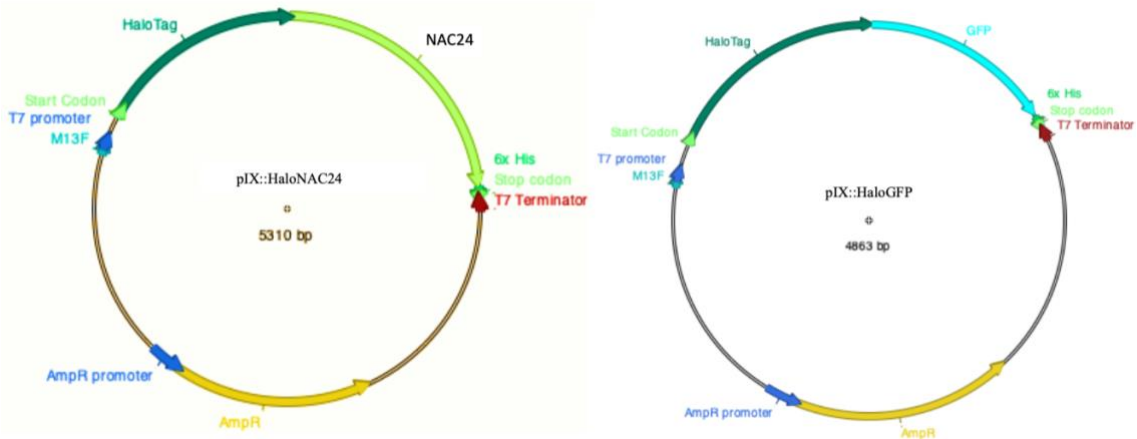

Figure 13: Genetic constructs to produce Halo-NAC24 and Halo-GFP in vitro. *(1)* pIX::HaloNAC24 *plasmid (2) p*IX::HaloGFP *plasmid. The constructs were obtained by Gateway recombination cloning. Both constructs consist of the* T7 *promoter (royal blue), a* HaloTag *DNA sequence (dark green),* NAC24 *ORF (green) or* GFP *ORF (light blue) and a* T7 *terminator (Red).*

Both plasmids were controlled by restriction with AatII enzyme (Figure 14).

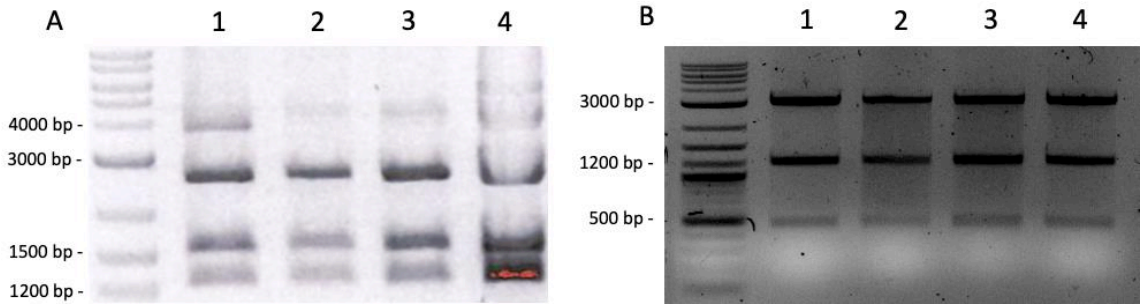

*Figure 14: (A) Control restriction of several p*IX::HaloNAC24 *plasmid preparations with AatII. Four fragments are visible and three of 2531, 1550 bp and 1229 bp are expected and visible. The fourth band at 4000 bp probably corresponds to partial digestion. (B) Control restriction of several pIX::HaloGFP plasmids with ApaLI. Three fragments are visible as expected: 3120, 1246 and 497 bp. On the left, the NEB 2-Log ladder was used.*

3.1.5. *In vitro* Halo-tagged protein synthesis

Using the TnT coupled transcription/translation system from wheat germ extract (Zhao *et al*., 2010), it was possible to transcribe and translate the pIX::HaloNAC24 and the pIX::HaloGFP into proteins in just over two hours. The proteins produced were checked by Western blot using anti-α-Halo antibodies and a single band with the appropriate molecular mass was detected for Halo-Nac24 and Halo-GFP (Figure 15, lanes A).

3.1.6. Binding of Halo-tagged proteins to magnetic beads

Magne®HaloTag® beads were washed several times with a PBS + NP40 solution in a 0,5 mL tube before adding the protein reaction mixture. The beads and proteins were rotated on a vertical rotator (14 rpm) for one hour at 25°C to ensure maximum binding of the Halo-NAC24 or Halo-GFP to the magnetic beads. Next, the supernatant was recovered with a magnetic rack and used for the quality control (QC) analysis (Figure 15, lanes B), and the beads were washed to remove unbound contaminants. Since some proteins had bound to the magnetic beads, the supernatant should contain less proteins than before binding. This was observed on the Western blot using the anti α-Halo antibody for both Halo-NAC24 and Halo-GFP where a reduced signal was detected after contact with the beads.

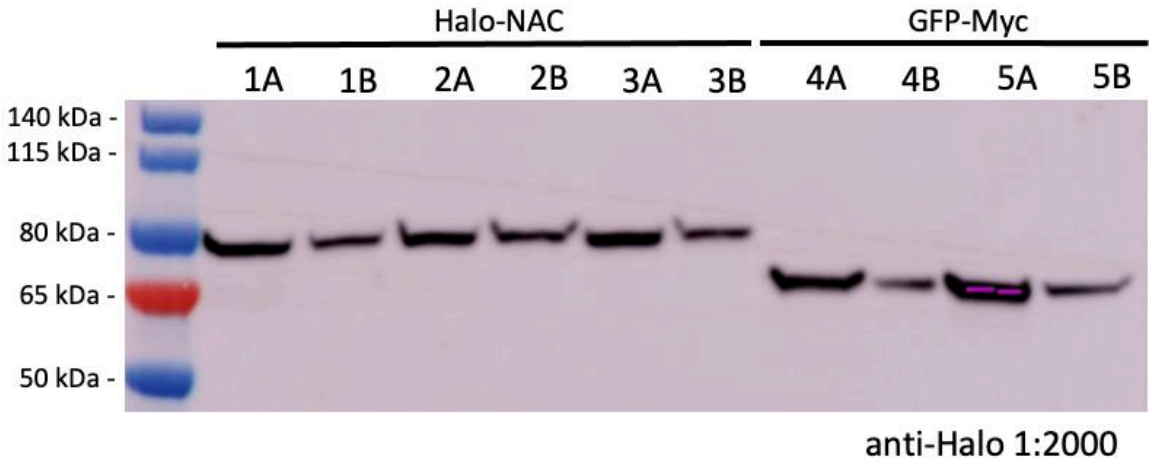

Figure 15: Quality control analysis of the protein binding of HaloTag fusion proteins after incubation with the Magne®HaloTag® Beads. Three replicates of each protein were in vitro *produced. The gel was loaded with Halo-NAC (1, 2 and 3) and Halo-GFP (4 and 5) samples before (A) and after (B) incubation with the beads.. The molecular mass markers are shown on the left.*

3.1.7. Binding of DNA libraries to Halo-tagged proteins

The different DNA libraries (1000 ng) were then added into the proteins and magnetic bead mix, and the samples were rotated for one hour at 25°C. To reduce the bias between samples, each Halo-NAC24 sample was brought in contact with the same DNA pool as a Halo-GFP sample. The initial protocol indicated using only 30-100 ng of DNA per sample

for *A. thaliana* which has a small genome (135 Mb). As the maize genome is 2365 Mb long, we decided to use 1000 ng instead, to ensure a similar number of genome copies in the reaction. After washes, the DNA was recovered by heating the magnetic beads at 98°C for 10 minutes, as the proteins remained bound to the beads only the DNA was recovered.

3.1.8. PCR amplification and indexing

The recovered DNA was then amplified in a PCR reaction for 30 cycles which should result in a higher DNA concentration, while maintaining a low bias. Indexing primers from the NEBNext Multiplex Oligos for Illumina kit were added to the reaction mix, along with DMSO to reduce the formation of secondary structures. The amplicon size was checked on agarose gel (Figure 16) and the remaining solution was purified on column using the MinElute PCR Purification Kit. The agarose gel showed that the amplicons have the correct sizes (100-300 bp), and the signal intensity of the samples was stronger than the negative control, where only the primers were added in the PCR reaction, indicating that the DNA was indeed amplified. As a final verification, DNA concentration was measured with a NanoDrop spectrophotometer to ensure that at least 40 ng DNA of good purity remained. The concentration of each sample was well above this range. The samples were finally sent to Microgen Bioproducts for Illumina sequencing.

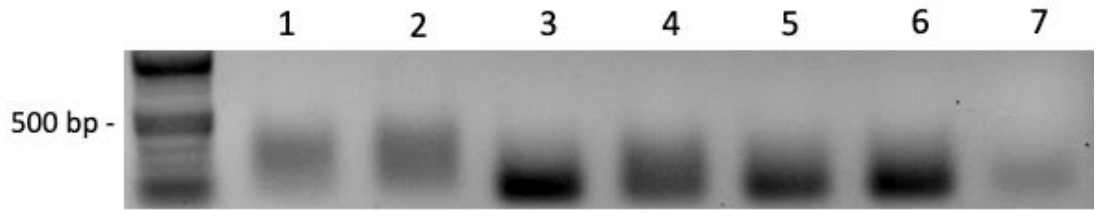

Figure 16: Agarose gel of PCR amplified samples. (1) Halo-NAC24 sample 1 (from gDNA A), (2) Halo-GFP sample 1 (from gDNA A), (3) Halo-NAC24 sample 2 (from gDNA B), (4) Halo-GFP sample 2 (from gDNA B), (5) Halo-NAC24 sample 3 (from gDNA C), (6) Halo-GFP sample 3 (from gDNA C), (7) Amplified sample with H_2O instead of DNA used as negative control. Samples using the same gDNA library (1-2, 3-4 and 5-6) have similar sizes and all show a stronger signal than the negative control.

3.2. Obtaining black Mexican sweet (BMS) maize suspension cells overexpressing *NAC24* or *GFP*

Stable cell lines overexpressing *NAC24* could provide a wealth of information, as various functional studies could be done on these systems. Moreover, *in vivo* studies such as ChIP-seq would also be possible.

3.2.1. Plasmid constructs

To perform ChIP-seq studies, one of the most important steps is immunoprecipitation and highly specific and effective antibodies are therefore extremely important (Kidder *et al*., 2011). NAC TFs possess strong homology between members, making it difficult to precipitate the target TF alone. It was therefore decided to proceed with two different epitope tags: the FLAG tag (DYKDDDDK) and the Myc tag (EQKLISEEDL). These tags have already been used to characterize NAC TFs in ChIP-seq experiments (Chung *et al*., 2018; Ren *et al*., 2021). The aim was to obtain two different plasmids, one expressing NAC24-Myc and the other expressing NAC24-FLAG, express the proteins, and determine by Western blot which anti-tag antibodies is the most specific and bind well to the fusion proteins. Since, for DAP-seq, GFP was used as negative control, we also used it for ChIP-seq, but we fused it with a NLS (MQPSLKRMKIEPSSQP) to address the GFP to the nucleus, where NAC24 acts (J. Lu *et al*., 2021; Maistriaux, 2021)

The genetic constructs were prepared using the Golden Gate MoClo Plant Tool Kit (Engler *et al*., 2014) and are shown in Figure 17. Each plasmid contains a kanamycin resistance cassette to select the transformed BMS cells on selective media. The encoded NAC24 protein was fused to the tags at its C-terminus. This position was chosen because the N-terminal sequence contains the NAC domain with its DNA binding capabilities. Finally, a cassette encoding the mCherry fluorescent protein was inserted, and is used to detect the cell lines expressing the transgenes.

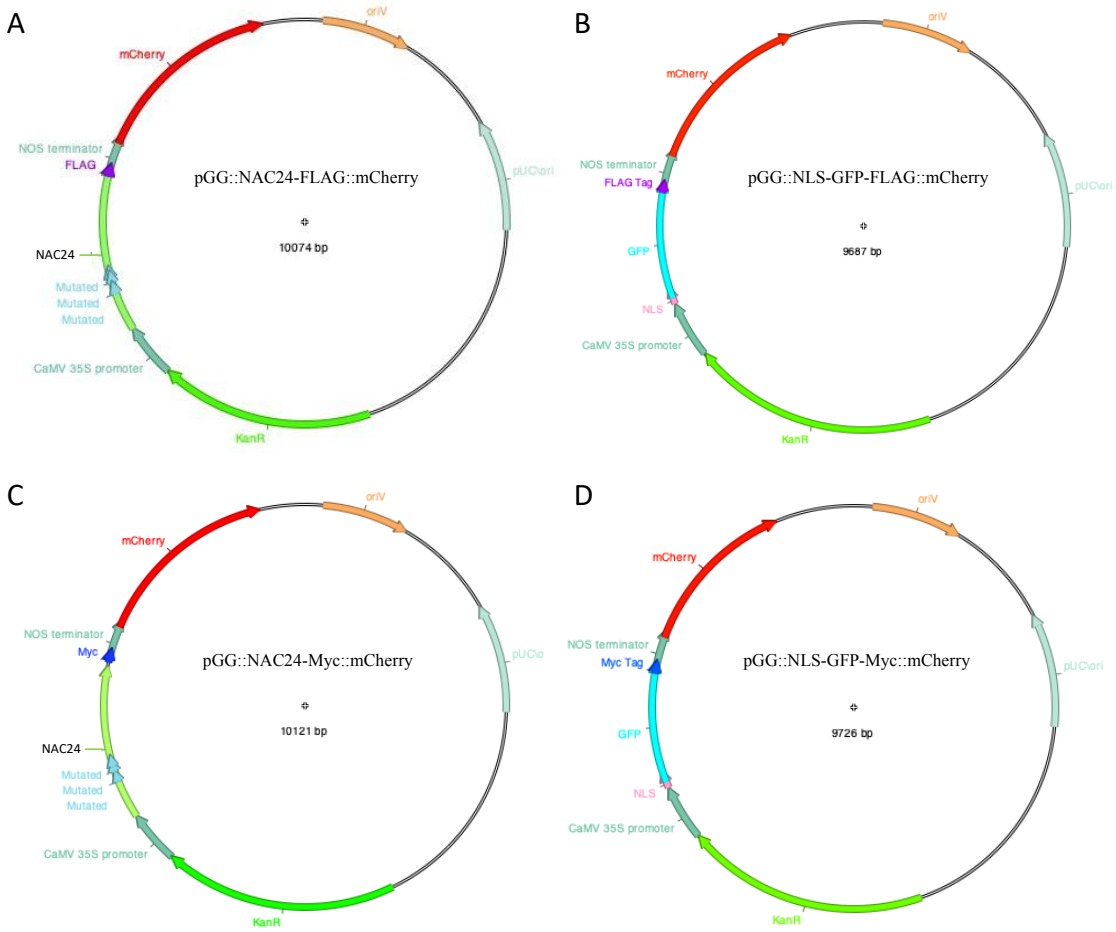

Figure 17: Genetic constructs to produce NAC24-FLAG, GFP-FLAG, NAC24-Myc and GFP-Myc in BMS cells. (A) pGG::NAC24-FLAG::mCherry, (B) pGG::NLS-GFP-FLAG::mCherry, (C) pGG::NAC24-Myc::mCherry, (D) pGG::NLS-GFP-Myc::mCherry. Each plasmid contains a kanamycin resistance cassette (neon green), a CaMV 35S *promoter (greyish blue), either* NAC24 *or* GFP *fused to a NLS (respectively light green or neon blue), either a FLAG tag (purple) or a Myc tag (royal blue), a* NOS *terminator (greyish blue) and an* mCherry *cassette (red).*

To verify that the plasmids were correctly constructed, control restrictions were performed and the inserts sequenced to verify that all parts were in frame with each other (Figure 18).

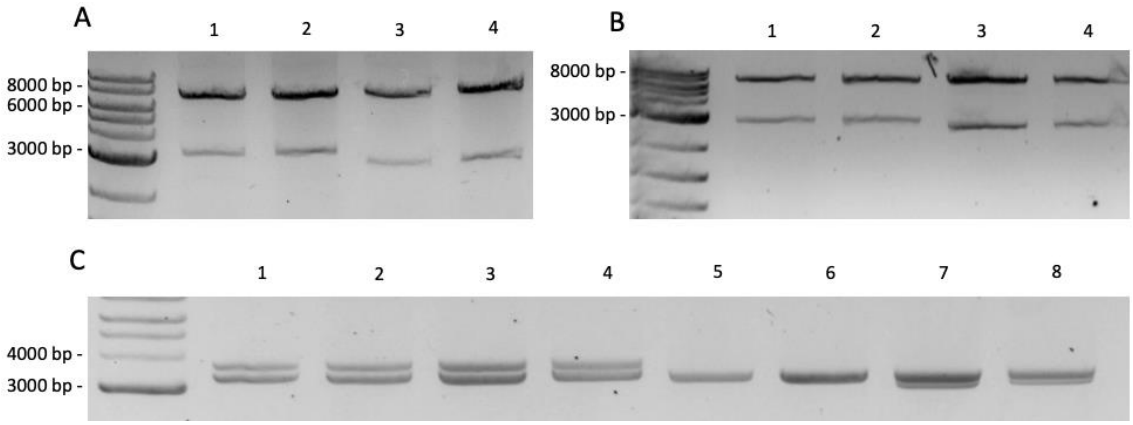

Figure 18: (A) Control restriction of pGG::NAC24-FLAG::mCherry *(A1 and A2) and* pGG::NLS-GFP-FLAG::mCherry *(A3 and A4) with AhdI. Two fragments of expected size are visible: 3132 bp and 6942 bp for A1 and A2 and 2745 bp and 6942 bp for A3 and A4. (B) Control restriction of* pGG::NAC24-Myc::mCherry *(B1 and B2) and* pGG::NLS-GFP-Myc::mCherry *(B3 and B4) with AhdI. Two fragments of expected size are visible: 3179 bp and 6942 bp for B1 and B2 and 2784 bp and 6942 bp for B3 and B4 (C) Control restriction of* pGG::NAC24-FLAG::mCherry *(C1 and C2),* pGG::NAC24-Myc::mCherry *(C3 and C4),* pGG::NLS-GFP-FLAG *(C5 and C6) and* pGG::NLS-GFP-Myc::mCherry *(C7 and C8) with ApaLI. Three fragments are visible as expected 3222, 3224, and 3628 bp (C1 and C2); 3222, 3224, and 3675 bp (C3 and C4); 3222, 3224, and 3628 bp (C5 and C6); 3222, 3224, and 3280 bp (C7 and C8). On the left of the gels the NEB 2-Log ladder was used.*

3.2.2. Transient expression in *Nicotiana benthamiana*

The functionality of the plasmids was tested by transient expression in *N. benthamiana* leaves before stable expression in the BMS cell lines. *Agrobacterium tumefaciens* infiltration of *N. benthamiana* leaves is a technique to express a transgene and detect the proteins of interest within a few days (Reed & Osbourn, 2018). Usually, this detection is done by Western blot.

Electrocompetent *A. tumefaciens* cells were transformed with either *pGG::NAC24-FLAG::mCherry*, *pGG::NLS-GFP-FLAG::mCherry*, *pGG::NAC24-Myc::mCherry* or pGG::NLS-GFP-Myc::mCherry plasmid. After plasmid DNA purification and its verification by digestion with restriction enzymes, *A. tumefaciens* were *agro*inflitrated into two or three *N. benthamiana* leaves from 4-week-old plants. Six days later, leaf samples were collected and homogenized, and the total soluble proteins were extracted using a buffer supplemented with NaCl in order to recover nuclear proteins (see Materials

and Methods). Protein concentration was measured using the Bradford method and the expression of the protein of interest was evaluated by Western blotting using antibodies raised against either the FLAG tag or the Myc tag (Figure 19.A, B and C). To check mCherry expression, anti-mCherry antibodies were used (Figure 19.D). Those Western blots appear slightly higher than they should due to an unknown problem which was raised by several people in the laboratory.

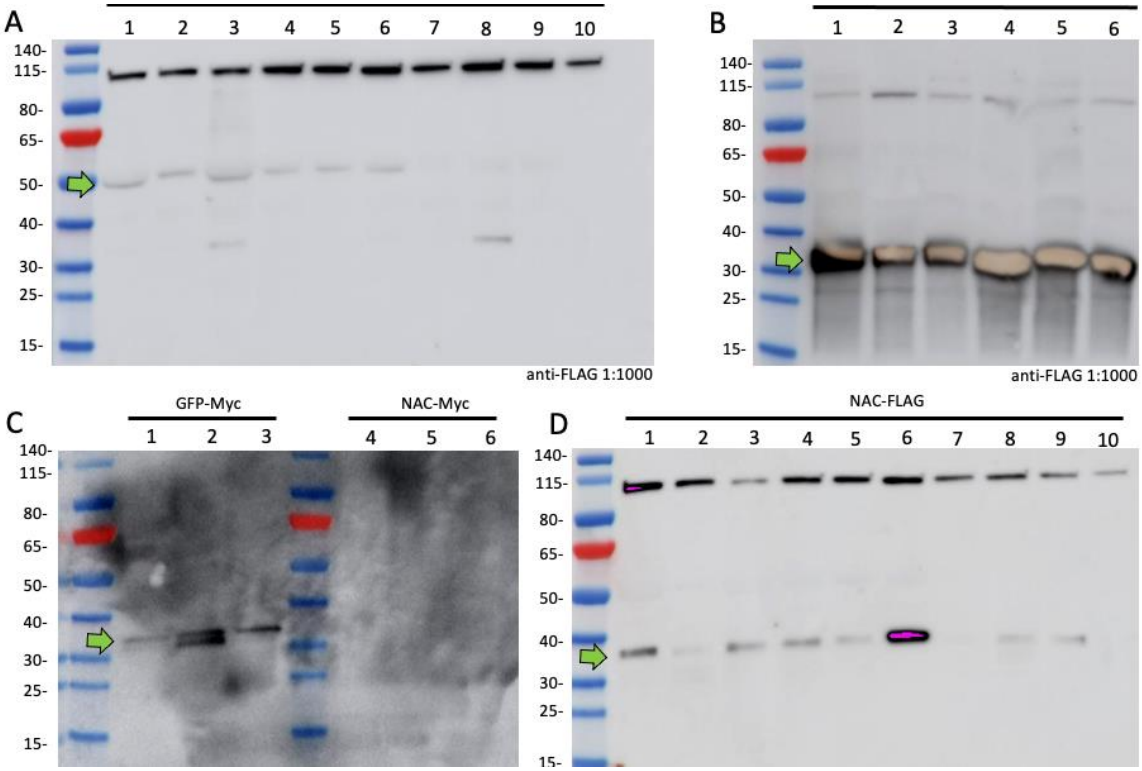

Figure 19: Western blot anti-FLAG, anti-MYC and anti-mCherry antibodies for visualization of NAC-FLAG, GFP-FLAG, NAC-Myc, GFP-Myc and mCherry in protein extracts from agroinfiltrated N. benthamiana *leaves. Proteins were extracted six days after agroinfiltration. While each leaf was infiltrated, the proteins are not visible in all extracts and no negative control was made. GFP has a molecular mass of ~27 kDa, NAC24 is 42 kDa, mCherry is 26 kDa, FLAG is 1 kDa and Myc is 1 kDa. An unspecific band of ~105 kDa is visible on gels (A), (B) and (D). Due to an unknown issue with some Western blots, the bands appear ~6 kDa higher than they should. The expected bands are indicated with a green arrow. The molecular mass markers are shown on the left.*

*(A) NAC24-FLAG detection in p*GG::NAC24-FLAG::mCherry *infiltrated leaves, expected molecular mass: 43 kDa. A band probably corresponding to NAC24 is visible at ~50 kDa in the lanes 1 to 6 as well as a possible truncated protein band at ~35 kDa in lanes 2 and 8, which was hypothesized to be due to the presence of a second ATG in the* NAC24 *sequence (Capuano, 2023).*

*(B) NLS-GFP-FLAG detection in p*GG::NLS-GFP-FLAG::mCherry *infiltrated leaves, expected molecular mass: 28 kDa. Bands around ~34 kDa probably corresponding to the protein are visible.*

*(C) NLS-GFP-Myc detection in p*GG::NLS-GFP-Myc::mCherry *infiltrated leaves and NAC24-Myc detection in p*GG::NAC24-Myc::mCherry *infiltrated leaves. Expected NLS-GFP-Myc molecular mass: 28 kDa. Bands around ~34 kDa probably corresponding to the protein are visible as well as a degradation band in the second lane. Expected NAC24-Myc molecular mass: 43 kDa. The bands corresponding to NAC24 are not visible.*

*(D) mCherry detection in p*GG::NLS-GFP-FLAG::mCherry *infiltrated leaves, expected molecular mass: 27 kDa. Bands around ~33 kDa probably corresponding to the protein are visible in all lanes except the seventh and tenth.*

The Western blots showed that the GFP-Myc was hardly visible (the membrane had to be exposed a long time to observe a signal), and NAC24-Myc was not detected. This was in contrast to the signals observed using the anti-FLAG antibodies, suggesting a better affinity for the FLAG-tagged proteins. Therefore, the FLAG constructs were chosen for BMS cells transformation. In addition, the *anti*-mCherry Western blot showed a signal at the expected size, indicating that the fluorescent protein was well expressed and could be used to identify transformed BMS cells.

3.2.3. Stable transformation of BMS using biolistics

Stable transformation of BMS cells was performed in order to perform ChIP-seq experiments and to study the impact of *NAC24* overexpression on the cell physiology in different growing conditions. Maize BMS suspension cell cultures are homogeneous, stably transformable by biolistics and protoplasts can be easily prepared to study the membrane osmotic water permeability, which could be useful to link NAC24 to the AQP ZmPIP2;5 abundance and activity (Moshelion *et al*., 2009). However, as obtaining transformed BMS lines was time consuming, we carried out the transformation, but were not able to characterize the obtained lines in the frame of this work.

Maxipreparations of the *pGG::NAC24-FLAG::mCherry* and *pGG::NLS-GFP-FLAG::mCherry* plasmids were used to coat gold particles, used to transform BMS cells by biolistics. BMS cells were collected from 9-day-old liquid culture and placed on a filter paper on MS plates. These cells were then bombarded with the gold beads using the

PDS-1000/He Biolistic particle bombardment delivery system (Bio-Rad, Hercules, CA, USA) in sterile conditions. After three days, the cells were transferred on a plate containing the antibiotic, and this was repeated every two weeks for two months. After this growth period, growing cells were harvested and placed again on selective medium but without the filter paper. After three months of growth, two plates of transformed cells were identified with the mCherry fluorescence (Figure 20), one expressing NAC24-FLAG and on expressing GFP-FLAG. Two NAC24-FLAG fluorescent calli were then transferred to liquid medium for growth (Figure 21). As explained above, due to time constraints, these cells could not be further screened via Western blot.

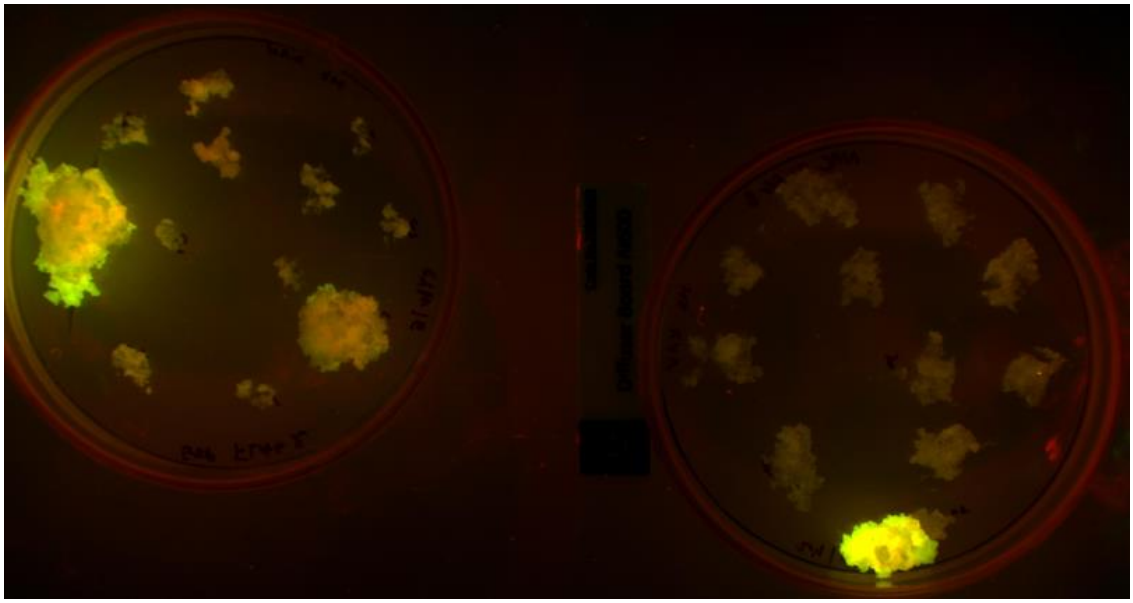

Figure 20: Amersham Imager 600 images of transfected BMS cells. On the right, a plate containing BMS calli transformed with the pGG::NAC24-FLAG::mCherry *plasmid. The two big fluorescent calli were selected to be placed in liquid culture for further screening. On the left, a plate containing BMS calli transformed with the* pGG::NLS-GFP-FLAG::mCherry *plasmid. The mCherry fluorescent signal appears in green.*

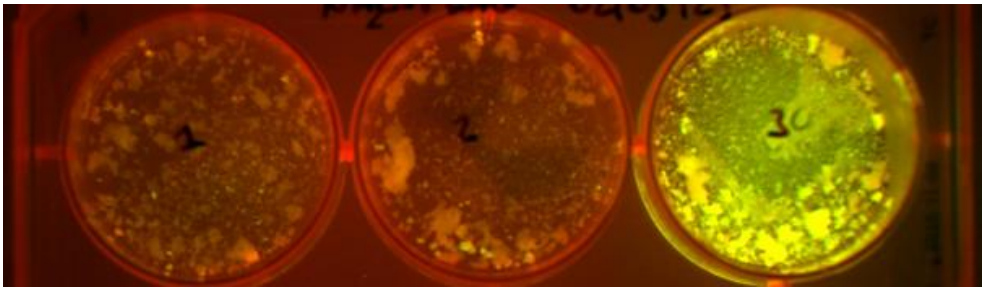

Figure 21: Amersham Imager 600 images of transfected BMS cells in liquid medium in a six-well plate. Two calli from the pGG::NAC24-FLAG::mCherry *plate were transferred to liquid medium for further growth and screening.The mCherry fluorescent signal appears in green.*

4. Discussion & Perspectives

An eQTL study performed by Laurie Maistriaux identified *NAC24* TF as a putative regulator of *ZmPIP2;5* AQP gene expression. This was confirmed by Estelle Teirlinckx and we were interested in identifying the other target genes of NAC24 and its binding motifs. To this aim, we set up a DAP-seq experiment with the NAC24 protein. In addition, stable lines of BMS suspension cells expressing NAC24-FLAG and GFP-FLAG were obtained to further conduct ChIP-seq experiments as well as other potential physiological studies.

4.1. Adjustments to DAP-seq protocol

To implement the original DAP-seq protocol (Bartlett *et al*., 2017) in the host laboratory, some adaptations were made to cope with the absence of certain equipment (i.e., the Covaris S2 ultrasonicator needed for gDNA fragmentation) or kits that had been modified since the article was published (i.e., the End-Repair Kit becoming the Fast End-Repair Kit). We also modified the gDNA cleaning step. Indeed, after gDNA extraction and fragmentation in a sonication bath, a cleaning of the gDNA was necessary, but only 20 to 25% of gDNA was recovered compared to the 80 to 90% recovery other experimenters obtained in the host laboratory. We adapted the amount of gDNA used for sonication, the conditions of the sonication and the ethanol percentage used for the cleaning step. This optimization of the protocol allowed us to achieve 30 to 35% recovery on average. The discrepancy between this and the other experimenter's recovery rate was hypothesized to be due to the type of tissue used. Indeed, as reported by Varma *et al*. (2007), contaminants such as polysaccharides are difficult to detect in gDNA samples and difficult to remove. Besides, they give false indications of the presence of high amounts of gDNA as explained by Varma *et al*. (2007). Primary roots contain high amounts of starch amongst others, which can explain the difference as the other researchers extracted their gDNA from leaves. We thus decided to continue the experiment bearing in mind that the concentration of gDNA measured before the cleaning step was probably overestimated. This was confirmed as the recovery rates went up to 80-90% for the subsequent washing

steps. The remaining steps in the creation of DNA libraries followed the original protocol: an end-repair reaction, an A-tailing reaction, and a final adaptor ligation step.

To successfully conduct the DAP-seq protocol, plasmids expressing Halo-NAC24 and Halo-GFP were constructed and the proteins produced using an *in vitro* protein expression system. The Halo-tagged fusion proteins were then bound to HaloTag-binding magnetic beads, forming covalent bonds. The prepared DNA libraries were then added, mixed, and washed to ensure that only the DNA strands recognized by the protein remained attached. The DNA was released and amplified by PCR with specific primers. After purification, the solution was sent to Microgen Bioproducts for Illumina sequencing.

4.2. Analysis of DAP-seq results

As studied by O'Malley *et al*. (2016), NAC TFs showed a high success rate compared with 151 other *A. thaliana* TFs. At the time of writing, the DAP-seq sequencing results have not yet been received. The way in which the analysis could be done is thus presented here, adapted from the protocol developed by O'Malley *et al*. (2016). The sequencing reads will be mapped to the B73 genome sequence using bowtie2 (Langmead & Salzberg, 2012) with a post-processing filter that removes reads that have been mapped to multiple locations at once. Next, peak calling will determine which parts of the genome are enriched in reads and will be achieved using GEM peak caller (Y. Guo *et al*., 2012) with the B73 nuclear genome sequence. Next, quality control metrics will be calculated by the R package ChIPQC (Carroll *et al*., 2014). To compute the read coverage across the genome, deepTools (Ramírez *et al*., 2014) will be used. To link peaks to gene features and repeat regions, Genome Association Tester (Heger *et al*., 2013) will be used. In Malley *et al*. (2016), all these manipulations were done in the snakemake bioinformatics workflow engine (Köster & Rahmann, 2012). For motif discovery, GEM generally finds short motifs, whereas the meme-chip tool in the MEME suite discovers longer motifs (Machanick & Bailey, 2011). Of course, it will be necessary to collaborate with the LIBST bioinformatician to properly perform all these analyses. Thanks to this analysis, peaks at genome locations where NAC24 binds will be detected. From those peaks, the

targets and binding motifs will be deduced. Compared to NAC24 peaks, the GFP signal should be continuously flat, as it expects to bind non-specifically to the gDNA.

4.3. Expected DAP-seq results

As mentioned in the introduction, a genome-wide analysis classifies NAC24 as part of the NAM subfamily, which is related to shoot apical meristem, flower development and senescence. NAC24 also possesses ABRE, MBS and WRKY binding sites in its promoter region, indicating a link with abiotic stress response. Additionally, a study by Wang *et al*. (2020) showed that NAC24 was more expressed after drought stress and repressed after rewatering. This can provide insight into potential binding sites that can be expected from the DAP-seq analysis, such as sites linked to development, growth and drought stress.

Other target genes may be members of the *PIP* AQP subfamily, mostly located in the plasma membrane and generally functioning as water channels (Chaumont *et al*., 2001; Gomes *et al*., 2009). Indeed, an interaction between *PIP2;5* and NAC24 has already been demonstrated in the laboratory, and, recently, preliminary results indicated a transactivation of *ZmPIP2;9* by NAC24, although this has to be confirmed. In addition, NAC TFs share common expression patterns with AQPs in response to abiotic stresses and in some developmental processes (Afzal *et al*., 2016; Capuano, 2023; Nuruzzaman *et al*., 2010). Multiple occurrences between NACs and AQPs were reported in different species. In *Tamarix hispida,* direct binding of ThNAC12 to the *ThPIP2;5* AQP promoter leading to its activation in salt stress conditions was demonstrated (R. Wang *et al*., 2021). In rose, RhNAC100 binds to the promoter of *RhPIP1;1* and *RhPIP2;*1 (Pei *et al*., 2013), and in *prunus armeniaca*, coexpression of AQP and NAC genes was detected during dormancy as well as sprouting stages, an observation that could be linked to cold resistance (Capuano, 2023; S. Li *et al*., 2021). We expect to find fragment(s) of *ZmPIP2;5* promoter in the NAC24 DAP-seq sequencing data, which should help determining the still unknown NAC24 binding site(s). In addition, other AQP promoter fragments could be identified, placing NAC24 as a master regulator of AQPs.

4.4. Synergy between DAP-seq and ChIP-seq

DAP-seq is not an alternative to ChIP-seq. While both methods are quite similar in principle, they complement each other and bring different information on TF mechanisms. On one hand, the *in vitro* nature of the DAP-seq allows the protein to bind without interference from the cellular machinery, with the exception of DNA methylations (which can also be removed by ampDAP-seq). The TF binding profiles obtained by DAP-seq are valuable when characterizing open chromatin regions as well as direct *in vivo* binding (O'Malley *et al*., 2016). On the other hand, ChIP-seq has *in vivo* interference. TFs can be hindered by chromatin availability or by other protein bound to the target region. Conversely, another protein binding to the TF could induce changes in its 3D structure, which may change its binding characteristics (O'Malley *et al*., 2016).

In conclusion, peaks which are only present in DAP-seq generally indicate targets that are not available *in vivo,* while peaks that can only be observed in ChIP-seq are mostly explained by indirect binding. A combination of the two will bring high motif scores and better predictions (O'Malley *et al*., 2016).

To provide additional information to the DAP-seq results by performing ChIP-seq experiments, we choose to express a tagged version of *NAC24* in BMS cells. Therefore, plasmids were constructed using Golden Gate cloning to obtain a final plasmid containing a kanamycin resistance cassette, a cassette expressing either a tagged NAC24 or tagged GFP fused with a NLS sequence, and a mCherry cassette. The tags, either FLAG or Myc, were added to the N-terminal part of the proteins. After *agro*infiltration of these plasmids into *N. benthamiana* leaves, the different cassettes were correctly expressed. Furthermore, it indicated that the FLAG tag has a higher affinity for its antibody compared to Myc tag, which is an important factor for the efficiency of the ChIP-seq immunoprecipitation step. We therefore decided to proceed only with the FLAG tag constructs. These constructs were then biolistically introduced into BMS maize cells, which were then selected on selective medium.

4.5. NAC24 overexpressing BMS cells potential studies

Due to time constraints, the cell lines were not screened for the expression of GFP-FLAG and NAC24-FLAG, but the mCherry fluorescence indicated that the transformation was effective. We will characterize the obtained lines by Western blot for the protein production and analyze the genomic insertion by iPCR.

To confirm the DAP-seq results, qPCR can be performed during ChIP-seq on selected NAC24 targets found during the process, comparing the wild type and NAC24 (over)expressing cells. We will start with the *PIP2;5* promoter. In addition, other studies can be carried out on BMS cells overexpressing NAC24. Swelling assays is often used for AQP activity determination and we hypothesize that the permeability of the cells expressing NAC24 would be higher, as NAC24 is expected to induce PIP2;5 expression (Cavez *et al*., 2009; Moshelion *et al*., 2009; Pickard, 2008). Physiological tests such as studying cell growth under abiotic stress are another option.

5. Materials and methods

5.1. Materials

5.1.1. Media

5.1.1.1. Lysogeny broth

Lysogeny broth (LB) medium was used for *E. coli* culture. It contains 10 g/L tryptone, 10 g/L NaCl and 5 g/L yeast extract for liquid culture. Additionally, 15 g/L agar was added for solid medium. For selective media, either 100 mg/L of spectinomycin (LBS), carbenicillin (LBC), kanamycin (LBK) or ampicillin (LBA) was added. For blue/white screening, 40 mg/L IPTG and 40 mg/L X-Gal were added to the solid medium.

5.1.1.2. 2x Yeast extract and tryptone

2x Yeast extract and tryptone (2YT) medium was used for *A. tumefaciens* culture. It contains 16 g/L tryptone, 5 g/L NaCl, 10 g/L yeast extract and 0.4 g/L $MgSO_4$. Additionally, 15 g/L agar was added for solid medium. For selective media, 20 mg/L rifampicin, 40 mg/L gentamycin and 100 mg/L kanamycin were added (2YTRGK).

5.1.1.3. MS medium

Murashige and Skoog (MS) medium was used for culture of BMS maize cells culture. It contains 4.4 g/L Murashige and Skoog Basal Salts with minimal organics, 30 g/L sucrose, 0.2 g/L L-asparagine and 3 mg/L 2,4-Dichlorophenoxyacetic acid (2,4D) at pH 5.8 (KOH). Additionally, 9 g/L agar was added for solid medium. For selective media, 100 mg/L or 150 mg/L kanamycin was added.

5.1.1.4. Leaf infiltration medium

Leaf infiltration medium (10 mM MES, 10 mM $MgCl_2$ at pH 5.6 (KOH)) was used for *agro*infiltration.

5.1.1.5. Extraction medium

Extraction medium (60 mM Tris (pH 8), 250 mM sorbitol, 2 mM EDTA, 0.6% polyclar AT, DTT 10 mM, 1 mM PMSF 2 mg/L) supplemented with two protease inhibitor cocktails (pepstatin and chymostatin; leupeptin, aproptinin and antipain) was used for protein extraction from *N. benthamiana* leaves.

5.1.2. Cellular strains

5.1.2.1. *E. coli*

The electrocompetent JM109 and thermocompetent TOP10 *E. coli* strains were used for amplification and selection of the plasmids. Bacteria were grown in LB medium in a dark room at 37°C.

5.1.2.2. A. tumefaciens

The electrocompetent LBA4404VirG *A. tumefaciens* strain was used for *N. benthamiana* leaf infiltration. This strain has the rifampicin resistance gene *TiAch5* in its genome. It possesses two plasmids: the disarmed Ti plasmid PAL4404 and the pBBR1MCS-virG54D, which was mutated for constitutive expressed VirG virulence. The pBBR1MCS-virG54D plasmid contains a gentamycin resistance gene for selection. Bacteria were grown in 2YTRGS medium in a dark room at 28°C.

5.1.3. Plant culture

5.1.3.1. Maize seeds

The *Zea mays* B73 inbred line was used for gDNA extraction. The seeds were sterilized with a 50% (v/v) bleach solution for 5 min and rinsed 5 times with water. Then, the seeds were germinated between moistened paper towels and incubated at 28°C in the dark for three days.

5.1.3.2. *N. benthamiana* seeds

N. benthamiana was used for transient expression using *agro*infiltration. The seeds were put for germination on humid potting soil in a growing chamber at 27°C. After a week, the seedlings were transferred to a rehydrated Jiffy® soil pellet. After the second week,

the growing plants were put in bigger pots and filled with soil. They were then placed in a 25°C growing chamber and watered daily.

5.1.3.3. BMS maize cells

The BMS suspension cell line was derived from the *Zea mays* Black Mexican Sweet variety, firstly developed by William Sheridan (Sheridan, 1975, 1982). For liquid culture BMS cells were grown in 50 mL MS medium in a 250 mL Erlenmeyer flask in the dark at 25°C agitated by a rotary shaker (90 rpm, Edmund Buhler GmbH). Every two weeks the liquid cultures were put in fresh medium (10 % v/v inoculum). To obtain liquid culture 5 mL of liquid BMS medium is introduced in an six-well plate and calli are disaggregated. After two weeks, the culture can be scaled to bigger volume.

5.1.4. Plasmids

5.1.4.1. p*IX-Halo::ccdB*

This plasmid was initially constructed by Yazaki *et al*. (2016)

and was used as expression clone in the Gateway cloning method (Katzen, 2007). It contained an ampicillin resistance gene *bla* for bacterial selection, a HaloTag cassette in 5' of the cDNA of interest insertion site and a *ccdB* sequence used as negative selection in Gateway cloning, which was flanked by attR1 and attR2 recombination sites for the LR reaction.

5.1.4.2. p*ENTR*::*NAC24*

The pENTR plasmid was used as entry clone in the Gateway cloning method (Katzen, 2007) and was procured from Thermo Fisher Scientific. It contains a kanamycin resistance gene for selection in *E. coli* and a *ccdB* sequence used as negative selection in Gateway cloning which is flanked by attL1 and attL2 recombination sites for the BP reaction. The BP reaction was made previously by Maxime Laurent, who inserted the mutated *NAC24* cDNA.

5.1.4.3. p*IX::HaloGFP*

This plasmid contains the *GFP* cassette from Gateway assembly fused to a HaloTag. It was assembled by Alice Berhin.

5.1.4.4. Golden Gate MoClo Plant Tool and Plant Parts Kits

These two collections of plasmids contain each 95 empty standardized genetic modules used for assembly using the Golden Gate cloning technique (Engler *et al*. 2014). In this study, the plasmids pAGM1287 (Level zero acceptor for coding sequences without stop codon with a spectinomycin resistance cassette for bacterial selection), pICH47742 (Level 1 acceptor for position 2 in forward orientation with carbenicillin resistance cassette for bacterial selection), pAGM4673 (Level 2 acceptor with a kanamycin resistance cassette for bacterial selection), pICH41766 (End-link 3 for assembling 3 level one part into a level 2 acceptor with a spectinomycin resistance cassette for bacterial selection) were used. For the Plant Parts kit, the plasmids pICH51277 (promoter (0.4 kb), 35s (Cauliflower Mosaic Virus) + 5'UTR, Ω (Tobacco Mosaic Virus)), pICH41421 (3'UTR, polyadenylation signal/terminator, *nos* terminator (*A. tumefaciens*)), pICSL50007 (C-terminal FLAG tag (3xFLAG octapeptide)) and pICSL50010 (C-terminal Myc tag (4x Myc)) were used.

5.1.4.5. pSN39p*YSL2-NLS-GFP-GUS-RC*

This plasmid contains the *NLS-GFP* cassette used for PCR amplification with custom primers for the Golden Gate assembly. It was constructed by Alice Berhin.

5.1.4.6. p*GGZmNAC24-2HA*

This plasmid contains the silently mutated *NAC24* cassette used for PCR amplification with custom primers for the Golden Gate assembly. It was constructed by Nicolas Capuano.

5.1.4.7. p*GGp35S-mCherry-tNos*

This level 1 plasmid contains an *p35S::mCherry::Tnos* cassette which was inserted as a cassette in third position in a level 2 plasmid. It was obtained from Marie Peeters.

5.1.4.8. p*GGpNOS-KanR-tOCS*

This level 1 plasmid contains a Kanamycin resistant cassette which was inserted as a cassette in first position in a level 2 plasmid. It was obtained from Marie Peeters.

5.1.5. Primers

Table 1: Primers used for DNA sequence cloning. 'P' indicates a 5' phosphate group

Name	Sequence (5' - 3')	Purpose
Lvl0_NAC24ns_F	ttggtctcaAATGGAAGCATCAGCAGCAGCAG	Cloning of NAC24 with overhangs from Golden Gate level 0 CDS1
Lvl0_NAC24ns_R	ggtctcacgaaccGACTTGGTACCCGCCGGCAGG	
Lvl-1_NLS-GFP_F	ttgaagacaaAATGCAGCCTTCTCTTAAACG	Cloning of NLS-GFP with overhangs for Golden Gate level 0 CDS1 cloning
Lvl-1_NLS-GFP_R	ttgaagacaacgaaccCTTGTACAGCTCGTCCATGC	
Y adaptor strand A	ACACTCTTTCCCTACACGACGCTCTTCCGATCT	Y adaptor for DAP-seq protocol
Y adaptor strand B	P-GATCGGAAGAGCACACGTCTGAACTCCAGTCAC	

5.2. Methods

5.2.1. DNA manipulation

5.2.1.1. Polymerase Chain Reaction (PCR) amplification

For amplification from a template, 1 to 20 ng of DNA template, 1.25 µL of 10 µM forward and reverse primers, 1 µL of 10 mM dNTPs, 0.25 µL of Q5® High-Fidelity DNA Polymerase, 5 µL of Q5® reaction buffer and 5 µL Q5® High GC Enhancer was added to a 25 µL reaction mix. The thermocycler was set to the appropriate program, depending on the primers and the length of the amplicon. The amplification was verified using gel electrophoresis.

Concerning the DNA amplification for the DAP-seq experiment, 25 µL of the eluted resulting DNA was added to 1 µL Phusion® High-Fidelity DNA Polymerase (2000 U/mL), 10 µL 5X Phusion® HF Buffer, 2.5 µL of 10 mM dNTPs, 2.5 µL of the 10 µM chosen sequencing primers mix from the NEBNext® Multiplex Oligos for Illumina® kit and 1.5 µL DMSO. Water was added to adjust the volume to 50 µL. The thermocycler was set to the following program: 2 min 30 seconds at 98°C, then the following steps

were repeated 30 times: 15 seconds at 98°C, annealing for 30 seconds at 60°C, amplifying for 2 min at 72°C. In the end, the mix was incubated for 10 min at 72°C and the amplification was verified using gel electrophoresis by putting 5 µL of the reaction on agarose gel.

5.2.1.2. Enzymatic control restriction

For control restrictions, 3 µL of DNA was added to 0.5 µL restriction enzyme, 2 µL reaction buffer and the volume was adjusted to 20 µL. The mix was incubated for 1 hour at 37°C and verified using gel electrophoresis.

5.2.1.3. Agarose gel electrophoresis

The gel was prepared by mixing TAE or TBE with 1 % (v/w) agarose and dissolving it by heating using a microwave oven. Midori Green Advance DNA Stain was added at a 1:20000 dilution. The gel was then cast in an appropriate mold with a comb and left to cool down and polymerize. When ready, the gel was placed into the electrophoresis equipment in either TAE or TBE buffer. The samples were mixed with 6X loading buffer and loaded on the gel, as well as 7 µL of 2-Log DNA ladder. The migration was set at 100 V for the appropriate time and the results were revealed under UV light (265 nm).

5.2.1.4. DNA extraction from agarose gel

This extraction was performed using the innuPREP DOUBLEpure Kit (Analytik Jena, Jena, Germany) according to the manufacturer's instruction.

5.2.1.5. Sequencing

The DNA fragments were sequenced using the Sanger method by Microsynth Seqlab, an external laboratory. The sequencing primer (30 pmol) was added to 480-1200 ng of plasmid DNA in a total volume of 12 µL.

5.2.1.6. Gateway recombination cloning

BP reaction

For the BP reaction, 150 ng of plasmid containing recombination sites was added to 150 ng of the pENTR plasmid and diluted to a total volume of 8 µL in TE buffer (pH 8). The solution was incubated overnight at RT with 2 µL of BP Clonase II enzyme mix. Samples were incubated for 10 min at 37°C with 1 µL of the proteinase K solution to terminate the reaction. The resulting plasmid was then transformed in thermocompetent *E. coli* for selection and amplification.

LR reaction

For the LR reaction, 150 ng of Entry clone was added to 150 ng of Destination vector (pIX-Halo:ccdB) and diluted to a total volume of 8 µL in TE buffer (pH 8). The solution was incubated overnight at RT with 2 µL of LR Clonase II enzyme mix. Samples were incubated for 10 min at 37°C with 1 µL of the proteinase K solution to terminate the reaction. The resulting plasmid was then transformed in thermocompetent *E. coli* and grown on LBA for selection and amplification.

5.2.1.7. Golden Gate Cloning

The Golden Gate technique uses type IIS (shifted) restriction enzymes (i.e., BsaI and BbsI) in order to facilitate a simultaneous and directed gene assembly of multiple DNA parts (Bird *et al*., 2022; Engler *et al*., 2008). These shifted enzymes recognize their restriction sites and cut next to it, creating 4 bp junction overhangs known as fusion sites, which can be designed to fit in a certain place in the construction. In this study, an *NLS-GFP* fragment containing fusion sites for level 0 assembly was generated by PCR and placed into a level 0 vector (pAGM1287) using Golden Gate. Next, this plasmid was inserted into a level 1 vector (pICH47742) between the promoter (pICH51277) and the tag (pICSL50007 or pICSL50010) followed by the terminator (pICH41421). For NAC24, the PCR fragment was directly inserted in this level 1 plasmid. For the level 2 vector (pAGM4673), the kanamycin resistance (pGGpNOS-KanR-tOCS) gene was placed in first position, the generated level 1 vector in second and the *mCherry* cassette (pGGp35S-mCherry-tNos) in third place.

For all reactions, 20 fmol of each required plasmid was added to 1.5 µL T4 DNA Ligase, 2.5 µL T4 ligase buffer (10X) and 1 µL of either BpiI or BbsI (depending on the cleaving sites needed). The volume was adjusted to 25 µL. The solution was inserted into a thermocycler for 50 cycles of 2 min at 37°C and 5 min at 16°C which cleaves then ligates the fragments. In the end, the temperature stays at 80°C for 10 min. After, the reaction, the plasmid was transformed in electrocompetent JM109 *E. coli* for amplification and selection. The destination vector for each level possesses a *LacZ* operon for blue/white screening and a resistance gene. For selection, they were grown on LBS/LBC/LBK with IPTG and X-Gal (growing white colonies were selected).

5.2.1.8. Transformation of *E. coli* by heat-shock

After the Gateway recombination, 10 µL of the reaction mix was transferred to 40 µL of TOP10 *E. coli* and left for 5 to 30 min on ice. The solution was then quickly incubated at 42°C for 45 s. After the shock, the cells were left on ice for 10 min and 300 µL of LB. After one hour of incubation at 37°C, 200 µL was spread on a LBA plate and incubated at 37°C overnight.

5.2.1.9. Transformation of *E. coli* by electroporation

After the ligation reaction, 10 µL of the reaction mix was desalted by filtering on a 0.025 µm VSWP Millipore filter placed over Milli-Q water for 10 min. Then 5 µL were transferred to 40 µL of JM109 *E. coli.* After mixing, the cells were transferred to an electroporation cuvette (0.1 cm) and transformed at 1750 V for approximately 4 ms. After the shock, 1 mL of LB was quickly transferred to the cuvette to recover the cells. After one hour of incubation at 37°C, 200 µL was spread on a LB plate containing the appropriate antibiotic and incubated at 37°C overnight.

5.2.1.10. Minipreparation of *E. coli* plasmid DNA

A colony from the LB plate was inoculated and incubated in 4 mL of selective LB medium for 16 h at 37°C. Extraction of the plasmid was done using the SmartPure DNA Purification Kit according to the manufacturer's instruction.

5.2.1.11. Maxipreparation of *E. coli* plasmid DNA

This maxiprep was performed using the Nucleobond AX-500 kit (Mackerey Nagel) according to the manufacturer's instruction.

5.2.2. *A. tumefaciens* infiltration of *N. benthamiana* leaves

5.2.2.1. Transformation of *A. tumefaciens* by electroporation

To transform *A. tumefaciens,* 2 µL of plasmid was mixed with 40 µL of electrocompetent LBA4404 virG cells. The cells were transferred to an electroporation cuvette (0.1 cm) and transformed at 1320 V for approximately 4 ms. After the shock, 1 mL of 2YT was quickly transferred to the cuvette to recover the cells. After incubating them at 28°C for one h, 200 µL of the solution was spread on a 2YTRGK plate and incubated at 28°C for 3 days.

5.2.2.2. Minipreparation of *A. tumefaciens* plasmid DNA

A. tumefaciens colony was inoculated in 10 mL 2YTRGK and incubated overnight at 28°C. Extraction of the plasmid was performed using the SmartPure DNA Purification Kit according to the manufacturer's instruction.

5.2.2.3. *Agro*infiltration of *N. benthamiana* leaves

Transformed *A. tumefaciens* colonies were streaked on a 2YTRGK plate, incubated at 28°C for 3 days, inoculated in 10 mL 2YTRGK and incubated overnight at 28°C. The optical density at 600 nm (OD_{600}) was measured and the cells diluted to obtain an OD_{600} of 0.8 in 10 mL. The cells were centrifuged at 3200 g for 10 min and the supernatant was discarded to resuspend the pellet in leaf infiltration medium to infiltrate 4-week-old *N. benthamiana* leaves on the abaxial side using a needleless syringe.

5.2.3. Protein analysis

5.2.3.1. *N. benthamiana* leaves protein extraction

Six days after infiltration, four disks (80 mg) were collected from the leaves, frozen in liquid nitrogen and grinded in 700 µL extraction medium in a glass tissue grinded size 22 on ice. The extract was centrifuged 5 min at 9000 g at 4°C. The recovered supernatant was centrifuged 15 min at 54000 rpm at 4°C in an Optima MAX Ultracentrifuge (Beckman-Coulter). The supernatant was quantified using the Bradford assay before conducting a Western blot.

5.2.3.2. Bradford assay

Samples were prepared by diluting 4 µL in 96 µL NaOH 0.1 N, 900 µL Bradford reagent (100 mg/L Coomassie brilliant blue G-250, 5% ethanol, 8.5% H_3PO_4) was added and the solution was incubated for 5 min. Standards of Bovine Serum Albumine (0 to 12 mg/L) 0.1 N NaOH were used for the calibration curve. A 96-well plate was used to measure the absorbance of 200 µL solution at 595 nm (SPECTROstar Nano BMG Labtech).

5.2.3.3. Western blot

For the analysis, samples (20 µg for proteins extracted from *N. benthamiana* leaves) were added to Laemli buffer 3X (240mM Tris HCl, 6% (w/v) SDS, 30% (w/v) glycerol, 0.05% (w/v) bromophenol blue, pH 6.8, 3% (w/v) DTT and 2 µg/mL protease inhibitor cocktails) and incubated for 10 min at 60°C. The samples were loaded in a precast gel (EUROGENTEC, 4-20%) as well as 7 µL Pageruler Prestained Protein Ladder (Thermo Fisher Scientific, Waltham, USA). The migration was done in MOPS buffer (50 mM Tris,50 mM MOPS, 1 g/L SDS and 0.3 g/L EDTA) at a constant 150 V and stopped when the blue staining exits the gel. The gel was then incubated and agitated for 10 min in transfer buffer (6 g/L Tris, 3 g/L glycine, 0.2 g/L SDS, and 20% (v/v) methanol). Transfer was done using the Trans-Blot Turbo kit (BioRad) according to the manufacturer's instruction. After the transfer, the membrane was placed in blocking buffer (PBS 1X, 1 mL/L Tween20, 5 g/L milk powder) and agitated for 60 min. The membrane was then transferred in a 50 mL Falcon tube and washed three times for 5 min in washing buffer (PBS 1X, 1 mL/L Tween20, 5 g/L milk powder) before being incubated for 60 min with the corresponding primary antibody diluted (1/1000 for anti-FLAG, anti-Myc and anti-

mCherry; 1/2000 for anti-Halo) in the washing buffer. Next, the membrane was washed three times for 5 min with the washing buffer and incubated for 60 min with the correct secondary antibody diluted (1/10 000 except for the DAP-seq QC analysis where 1/100 000 was used) in washing buffer. Before revealing, the membrane was washed three times for 5 min and incubated in luminol solution for 30 s in the dark. The membrane was revealed with the Amersham Imager 600.

5.2.4. DAP-seq

5.2.4.1. Genomic DNA extraction

Three-day-old maize seed's primary root was collected, cut into small pieces and immediately frozen into liquid nitrogen. The root was ground by a mortar and pestle into thin powder and approximately 120 mg of root was distributed in each tube. This extraction was performed using the Wizard® Genomic DNA Purification Kit (Promega). Initially, 1.2 mL Nuclei Lysis Solution was added. The following steps were processed according to the manufacturer's instruction.

5.2.4.2. DNA library preparation

First, 10000 – 20000 ng of gDNA was diluted in 135 µL elution buffer (EB) (Qiagen) and sonicated in a Elmasonic S 10 (H) (Elma) sonication bath for 20 min. To verify the size, 10 µL of sonicated was analyzed with agarose gel electrophoresis. A sample cleanup was performed on the remaining gDNA by adding 12.5 µL of 3M NaOAc and 312 µL 100% ethanol (at -20°C) and incubating at -80°C for an hour. The solution was centrifuged for 20 min at 20000 g (4°C). The supernatant was discarded and the pellet was washed with 1 mL 80% ethanol. The sample was centrifuged for 10 min at 20000 g at RT. The supernatant was carefully decanted, and the pellet was rehydrated with 44.5 µL EB overnight. The concentration was verified using a NanoDrop Spectrophotometer.

The following day, the End-repair reaction was performed using Fast DNA End Repair Kit (Thermofisher Scientific), according to the manufacturer's instructions. A second step of sample cleanup was performed with 5 µL NaOAc, 150 µL 100% (v/v) ethanol and

rehydrated in 32 µL EB. For the A-tailing reaction, 5 µL NEBuffer2 (NEB), 10 µL 1 mM dATP and 3 µL Klenow Fragment (3'-5' exo-; 5 U/µL) (NEB) was added and incubated at 37°C for 30 min. A third sample cleanup step was performed with 5 µL NaOAc, 150 µL 100% (v/v) ethanol and rehydrated in 30 µL EB. The adaptor ligation step requires 5 µL T4 DNA Ligase 10X Buffer, 10 µL of 30 µM Y adaptor primer mix and 5 µL T4 DNA Ligase (3 U/µL) (Promega) to be added and incubated at RT for 3 h. A fourth sample cleanup step was performed with 5 µL NaOAc, 150 µL 100% (v/v) ethanol and rehydrated in 32 µL EB. The DNA concentration of 2 µL of the sample was measured using the Qubit dsDNA HS Assay Kit (Life Technologies) according to the manufacturer's instruction in order to verify that enough DNA was still present to proceed to the next step.

5.2.4.3. *In vitro* protein expression

Protein production was done using the TnT® Coupled Wheat Germ Extract (Promega) according to the manufacturer's instruction using the Gateway Recombination produced plasmids. Incubation was performed for 2 h and 10 µL of the reaction was taken for later quality control (QC) analysis (Western blot analysis comparing the protein content before and after contact with the beads to observe a reduction in protein content due to binding to the beads).

5.2.4.4. DAP-seq experiment

For the experiment, 20 µL of Magne HaloTag Beads (Promega) per sample was transferred to a 1.5 mL tube. The tube was placed on a magnetic rack so that the buffer can be pipetted off once the beads have been drawn magnetically. Three times, 1 mL PBS+NP40 solution (PBS with 25% (v/v) NP40 (Thermofisher Scientific)) was added to the beads, mixed, and removed. After the washes, 20 µL per sample PBS+NP40 solution was added to the beads and 20 µL of beads solution was transferred to a 0.5 mL tube per sample. Additional 20 µL of PBS+NP40 solution as well as 40 µL expression reaction was added for a total of 80 µL. The tube was incubated while rotating at 25°C for an hour. The supernatant was removed and saved for later QC analysis by placing the tube on a

magnetic rack. Four washing steps were performed using 85 µL PBS+NP40 solution. The beads were resuspended in 40 µL PBS+NP40 solution and 1000 ng DNA library was added. The volume was adjusted to 80 µL with EB and the tube was incubated while rotating at 25°C for an hour. The supernatant was removed by placing the tube in a magnetic rack and the beads were washed at least five times with 85 µL PBS+NP40. The beads were resuspended in 26 µL EB and the tube was placed on a heating block at 98°C for 10 min and placed on ice for 5 min immediately afterwards. The 0.5 mL tube was placed on a magnetic rack and 25 µL of the supernatant was transferred to a PCR tube. A PCR was performed according to subsection 2.2.1.1. The PCR product was purified using the MinElute PCR Purification Kit (Qiagen) according to the manufacturer's instruction eluting in 21 µL. As final verification, 1 µL was measured with a NanoDrop spectrophotometer and the sample was sent to Microgen Bioproducts for Illumina sequencing.

5.2.5. Biolistic transformation of BMS cell lines

The day before the bombardment, 2 to 3 mL of 9-day-old BMS cells was placed on a n°4 Whatman filter paper (Fischer Scientific) and filtered using a Büchner funnel. The cells coated filter paper was then transferred to a MS medium plate. The bombardment was performed using 1000 ng maxipreps and the biolistic particle delivery system (PDS-1000/He from Bio-Rad) following the manufacturer's protocol. The BMS cells were placed in the lower half of the vacuum chamber in sterile conditions. Three days later, the filter paper was transferred to a fresh MS medium plate containing 100 mg/L kanamycin and replaced every two weeks. After 2 months, growing cells were harvested on placed on MS medium with 150 mg/L kanamycin without filter paper. After three months of growths, surviving cells were studied for fluorescence using the Amersham Imager 600. These fluorescent *calli* have been transferred to MS liquid medium containing 150 mg/L kanamycin for liquid culture.

6. References

Afzal, Z., Howton, T. C., Sun, Y., & Mukhtar, M. S. (2016). The Roles of Aquaporins in Plant Stress Responses. *Journal of Developmental Biology*, *4*(1), Article 1. https://doi.org/10.3390/jdb4010009

Aida, M., Ishida, T., Fukaki, H., Fujisawa, H., & Tasaka, M. (1997). Genes involved in organ separation in Arabidopsis : An analysis of the cup-shaped cotyledon mutant. *The Plant Cell*, *9*(6), 841-857. https://doi.org/10.1105/tpc.9.6.841

Amack, S. C., & Antunes, M. S. (2020). CaMV35S promoter – A plant biology and biotechnology workhorse in the era of synthetic biology. *Current Plant Biology*, *24*, 100179. https://doi.org/10.1016/j.cpb.2020.100179

Amendt, B. A., Sutherland, L. B., & Russo, A. F. (1999). Transcriptional Antagonism between Hmx1 and Nkx2.5 for a Shared DNA-binding Site *. *Journal of Biological Chemistry*, *274*(17), 11635-11642. https://doi.org/10.1074/jbc.274.17.11635

Bakshi, M., & Oelmüller, R. (2014). WRKY transcription factors. *Plant Signaling & Behavior*, *9*(2), e27700. https://doi.org/10.4161/psb.27700

Bartlett, A., O'Malley, R. C., Huang, S. C., Galli, M., Nery, J. R., Gallavotti, A., & Ecker, J. R. (2017). Mapping genome-wide transcription-factor binding sites using DAP-seq. *Nature Protocols*, *12*(8), Article 8. https://doi.org/10.1038/nprot.2017.055

Berezovski, M., Drabovich, A., Krylova, S. M., Musheev, M., Okhonin, V., Petrov, A., & Krylov, S. N. (2005). Nonequilibrium Capillary Electrophoresis of Equilibrium Mixtures : A Universal Tool for Development of Aptamers. *Journal of the American Chemical Society*, *127*(9), 3165-3171. https://doi.org/10.1021/ja042394q

Bian, Z., Gao, H., & Wang, C. (2020). NAC Transcription Factors as Positive or Negative Regulators during Ongoing Battle between Pathogens and Our Food Crops. *International Journal of Molecular Sciences*, *22*(1), 81. https://doi.org/10.3390/ijms22010081

Bienert, G. P., Bienert, M. D., Jahn, T. P., Boutry, M., & Chaumont, F. (2011). Solanaceae XIPs are plasma membrane aquaporins that facilitate the transport of many uncharged substrates. *The Plant Journal: For Cell and Molecular Biology*, *66*(2), 306-317. https://doi.org/10.1111/j.1365-313X.2011.04496.x

Bienert, G. P., & Chaumont, F. (2014). Aquaporin-facilitated transmembrane diffusion of hydrogen peroxide. *Biochimica Et Biophysica Acta*, *1840*(5), 1596-1604. https://doi.org/10.1016/j.bbagen.2013.09.017

Bird, J. E., Marles-Wright, J., & Giachino, A. (2022). A User's Guide to Golden Gate Cloning Methods and Standards. *ACS Synthetic Biology*, *11*(11), 3551-3563. https://doi.org/10.1021/acssynbio.2c00355

Blackwell, T. K., & Weintraub, H. (1990). Differences and Similarities in DNA-Binding Preferences of MyoD and E2A Protein Complexes Revealed by Binding Site Selection. *Science*, *250*(4984), 1104-1110. https://doi.org/10.1126/science.2174572

Bowser, M. T. (2005). SELEX : Just another separation? *Analyst*, *130*(2), 128-130. https://doi.org/10.1039/B412492H

Brent, R., & Ptashne, M. (1985). A eukaryotic transcriptional activator bearing the DNA specificity of a prokaryotic repressor. *Cell*, *43*(3, Part 2), 729-736.

https://doi.org/10.1016/0092-8674(85)90246-6

Bulyk, M. L., Gentalen, E., Lockhart, D. J., & Church, G. M. (1999). Quantifying DNA–protein interactions by double-stranded DNA arrays. *Nature Biotechnology*, *17*(6), Article 6. https://doi.org/10.1038/9878

Bulyk, M. L., Huang, X., Choo, Y., & Church, G. M. (2001). Exploring the DNA-binding specificities of zinc fingers with DNA microarrays. *Proceedings of the National Academy of Sciences*, *98*(13), 7158-7163. https://doi.org/10.1073/pnas.111163698

Byrt, C. S., Zhao, M., Kourghi, M., Bose, J., Henderson, S. W., Qiu, J., Gilliham, M., Schultz, C., Schwarz, M., Ramesh, S. A., Yool, A., & Tyerman, S. (2017). Non-selective cation channel activity of aquaporin AtPIP2;1 regulated by Ca2+ and pH. *Plant, Cell & Environment*, *40*(6), 802-815. https://doi.org/10.1111/pce.12832

Cao, K., Wei, Y., Chen, Y., Jiang, S., Chen, X., Wang, X., & Shao, X. (2021). PpCBF6 is a low-temperature-sensitive transcription factor that binds the PpVIN2 promoter in peach fruit and regulates sucrose metabolism and chilling injury. *Postharvest Biology and Technology*, *181*, 111681. https://doi.org/10.1016/j.postharvbio.2021.111681

Capuano, N. (2023). *Characterization and physiological relevance of ZmNAC24 transcription factor and its relation to ZmPIP2;9*.

Carey, J. (1991). [8] Gel retardation. In *Methods in Enzymology* (Vol. 208, p. 103-117). Academic Press. https://doi.org/10.1016/0076-6879(91)08010-F

Carroll, T. S., Liang, Z., Salama, R., Stark, R., & de Santiago, I. (2014). Impact of artifact removal on ChIP quality metrics in ChIP-seq and ChIP-exo data. *Frontiers in Genetics*, *5*. https://www.frontiersin.org/articles/10.3389/fgene.2014.00075

Casaretto, J. A., El-kereamy, A., Zeng, B., Stiegelmeyer, S. M., Chen, X., Bi, Y.-M., & Rothstein, S. J. (2016). Expression of OsMYB55 in maize activates stress-responsive genes and enhances heat and drought tolerance. *BMC Genomics*, *17*(1), 312. https://doi.org/10.1186/s12864-016-2659-5

Cavez, D., Hachez, C., & Chaumont, F. (2009). Maize Black Mexican sweet suspension cultured cells are a convenient tool for studying aquaporin activity and regulation. *Plant Signaling & Behavior*, *4*(9), 890-892. https://doi.org/10.4161/psb.4.9.9484

Chaumont, F., Barrieu, F., Wojcik, E., Chrispeels, M. J., & Jung, R. (2001). Aquaporins Constitute a Large and Highly Divergent Protein Family in Maize1. *Plant Physiology*, *125*(3), 1206-1215. https://doi.org/10.1104/pp.125.3.1206

Chaumont, F., & Tyerman, S. D. (2014). Aquaporins : Highly Regulated Channels Controlling Plant Water Relations. *Plant Physiology*, *164*(4), 1600-1618. https://doi.org/10.1104/pp.113.233791

Chen, M., Wang, Q.-Y., Cheng, X.-G., Xu, Z.-S., Li, L.-C., Ye, X.-G., Xia, L.-Q., & Ma, Y.-Z. (2007). GmDREB2, a soybean DRE-binding transcription factor, conferred drought and high-salt tolerance in transgenic plants. *Biochemical and Biophysical Research Communications*, *353*(2), 299-305. https://doi.org/10.1016/j.bbrc.2006.12.027

Chen, Q., Wang, Q., Xiong, L., & Lou, Z. (2011). A structural view of the conserved domain of rice stress-responsive NAC1. *Protein & Cell*, *2*(1), 55-63. https://doi.org/10.1007/s13238-011-1010-9

Chen, Y., Li, X., Xie, X., Liu, L., Fu, J., & Wang, Q. (2023). Maize transcription factor ZmNAC2 enhances osmotic stress tolerance in transgenic Arabidopsis. *Journal of Plant*

Physiology, *282*, 153948. https://doi.org/10.1016/j.jplph.2023.153948

Chun, I., Kim, H. J., Hong, S., Kim, Y.-G., & Kim, M.-S. (2022). Structural basis of DNA binding by the NAC transcription factor ORE1, a master regulator of plant senescence. *Plant Communications*, 100510. https://doi.org/10.1016/j.xplc.2022.100510

Chung, P. J., Jung, H., Choi, Y. D., & Kim, J.-K. (2018). Genome-wide analyses of direct target genes of four rice NAC-domain transcription factors involved in drought tolerance. *BMC Genomics*, *19*(1), 40. https://doi.org/10.1186/s12864-017-4367-1

Danielson, J. Å., & Johanson, U. (2008). Unexpected complexity of the Aquaporin gene family in the moss Physcomitrella patens. *BMC Plant Biology*, *8*(1), Article 1. https://doi.org/10.1186/1471-2229-8-45

Danino, Y. M., Even, D., Ideses, D., & Juven-Gershon, T. (2015). The core promoter : At the heart of gene expression. *Biochimica et Biophysica Acta (BBA) - Gene Regulatory Mechanisms*, *1849*(8), 1116-1131. https://doi.org/10.1016/j.bbagrm.2015.04.003

Das, P. M., Ramachandran, K., vanWert, J., & Singal, R. (2004). Chromatin immunoprecipitation assay. *BioTechniques*, *37*(6), 961-969. https://doi.org/10.2144/04376RV01

de Beer, T. A. P., Berka, K., Thornton, J. M., & Laskowski, R. A. (2014). PDBsum additions. *Nucleic Acids Research*, *42*(D1), D292-D296. https://doi.org/10.1093/nar/gkt940

Di Giorgio, J. A. P., Bienert, G. P., Ayub, N. D., Yaneff, A., Barberini, M. L., Mecchia, M. A., Amodeo, G., Soto, G. C., & Muschietti, J. P. (2016). Pollen-Specific Aquaporins NIP4;1 and NIP4;2 Are Required for Pollen Development and Pollination in Arabidopsis thaliana. *The Plant Cell*, *28*(5), 1053-1077. https://doi.org/10.1105/tpc.15.00776

Diao, P., Chen, C., Zhang, Y., Meng, Q., Lv, W., & Ma, N. (2020). The role of NAC transcription factor in plant cold response. *Plant Signaling & Behavior*, *15*(9), 1785668. https://doi.org/10.1080/15592324.2020.1785668

Engler, C., Kandzia, R., & Marillonnet, S. (2008). A One Pot, One Step, Precision Cloning Method with High Throughput Capability. *PLOS ONE*, *3*(11), e3647. https://doi.org/10.1371/journal.pone.0003647

Engler, C., Youles, M., Gruetzner, R., Ehnert, T.-M., Werner, S., Jones, J. D. G., Patron, N. J., & Marillonnet, S. (2014). A Golden Gate Modular Cloning Toolbox for Plants. *ACS Synthetic Biology*, *3*(11), 839-843. https://doi.org/10.1021/sb4001504

Erenstein, O., Jaleta, M., Sonder, K., Mottaleb, K., & Prasanna, B. M. (2022). Global maize production, consumption and trade : Trends and R&D implications. *Food Security*, *14*(5), 1295-1319. https://doi.org/10.1007/s12571-022-01288-7

Ernst, H. A., Nina Olsen, A., Skriver, K., Larsen, S., & Lo Leggio, L. (2004). Structure of the conserved domain of ANAC, a member of the NAC family of transcription factors. *EMBO reports*, *5*(3), 297-303. https://doi.org/10.1038/sj.embor.7400093

Fan, K., Wang, M., Miao, Y., Ni, M., Bibi, N., Yuan, S., Li, F., & Wang, X. (2014). Molecular Evolution and Expansion Analysis of the NAC Transcription Factor in Zea mays. *PLOS ONE*, *9*(11), e111837. https://doi.org/10.1371/journal.pone.0111837

FAOSTAT. (2021). https://www.fao.org/faostat/en/#home

Fields, S. (2009). Interactive learning : Lessons from two hybrids over two decades. *PROTEOMICS*, *9*(23), 5209-5213. https://doi.org/10.1002/pmic.200900236

Fields, S., & Song, O. (1989). A novel genetic system to detect protein–protein interactions. *Nature*, *340*(6230), Article 6230. https://doi.org/10.1038/340245a0

Fox, A. R., Maistriaux, L. C., & Chaumont, F. (2017). Toward understanding of the high number of plant aquaporin isoforms and multiple regulation mechanisms. *Plant Science*, *264*, 179-187. https://doi.org/10.1016/j.plantsci.2017.07.021

Fried, M., & Crothers, D. M. (1981). Equilibria and kinetics of lac repressor-operator interactions by polyacrylamide gel electrophoresis. *Nucleic Acids Research*, *9*(23), 6505-6525. https://doi.org/10.1093/nar/9.23.6505

Fried, M. G. (1989). Measurement of protein-DNA interaction parameters by electrophoresis mobility shift assay. *ELECTROPHORESIS*, *10*(5-6), 366-376. https://doi.org/10.1002/elps.1150100515

Fried, M. G., & Garner, M. M. (1998). The Electrophoretic Mobility Shift Assay (EMSA) for Detection and Analysis of Protein-DNA Interactions. In D. Tietz (Éd.), *Nucleic Acid Electrophoresis* (p. 239-271). Springer. https://doi.org/10.1007/978-3-642-58924-9_10

Galas, D. J., & Schmitz, A. (1978). DNAase footprinting a simple method for the detection of protein-DNA binding specificity. *Nucleic Acids Research*, *5*(9), 3157-3170. https://doi.org/10.1093/nar/5.9.3157

Garner, M. M., & Revzin, A. (1981). A gel electrophoresis method for quantifying the binding of proteins to specific DNA regions : Application to components of the Escherichia coli lactose operon regulatory system+. *Nucleic Acids Research*, *9*(13), 3047-3060. https://doi.org/10.1093/nar/9.13.3047

Garner, M. M., & Revzin, A. (1986). The use of gel electrophoresis to detect and study nucleic acid—Protein interactions. *Trends in Biochemical Sciences*, *11*(10), 395-396. https://doi.org/10.1016/0968-0004(86)90149-0

Gerasimavicius, L., Livesey, B. J., & Marsh, J. A. (2022). Loss-of-function, gain-of-function and dominant-negative mutations have profoundly different effects on protein structure. *Nature Communications*, *13*(1), Article 1. https://doi.org/10.1038/s41467-022-31686-6

Gerbeau, P., Güçlü, J., Ripoche, P., & Maurel, C. (1999). Aquaporin Nt-TIPa can account for the high permeability of tobacco cell vacuolar membrane to small neutral solutes. *The Plant Journal*, *18*(6), 577-587. https://doi.org/10.1046/j.1365-313x.1999.00481.x

Gerstle, J. T., & Fried, M. G. (1993). Measurement of binding kinetics using the gel electrophoresis mobility shift assay. *ELECTROPHORESIS*, *14*(1), 725-731. https://doi.org/10.1002/elps.11501401115

Gilmour, D. S., & Lis, J. T. (1984). Detecting protein-DNA interactions in vivo : Distribution of RNA polymerase on specific bacterial genes. *Proceedings of the National Academy of Sciences*, *81*(14), 4275-4279. https://doi.org/10.1073/pnas.81.14.4275

Gilmour, D. S., & Lis, J. T. (1985). In Vivo Interactions of RNA Polymerase II with Genes of Drosophila melanogaster. *Molecular and Cellular Biology*, *5*(8), 2009-2018. https://doi.org/10.1128/mcb.5.8.2009-2018.1985

Gomes, D., Agasse, A., Thiébaud, P., Delrot, S., Gerós, H., & Chaumont, F. (2009). Aquaporins are multifunctional water and solute transporters highly divergent in living organisms. *Biochimica et Biophysica Acta (BBA) - Biomembranes*, *1788*(6), 1213-1228. https://doi.org/10.1016/j.bbamem.2009.03.009

Gonzalez, D. H. (2015). *Plant Transcription Factors : Evolutionary, Structural and Functional Aspects*. Academic Press.

Gopinath, S. C. B. (2007). Methods developed for SELEX. *Analytical and Bioanalytical Chemistry*, *387*(1), 171-182. https://doi.org/10.1007/s00216-006-0826-2

Greve, K., La Cour, T., Jensen, M. K., Poulsen, F. M., & Skriver, K. (2003). Interactions between plant RING-H2 and plant-specific NAC (NAM/ATAF1/2/CUC2) proteins : RING-H2 molecular specificity and cellular localization. *Biochemical Journal*, *371*(Pt 1), 97-108. https://doi.org/10.1042/BJ20021123

Grotewold, E., Drummond, B. J., Bowen, B., & Peterson, T. (1994). The myb-homologous P gene controls phlobaphene pigmentation in maize floral organs by directly activating a flavonoid biosynthetic gene subset. *Cell*, *76*(3), 543-553. https://doi.org/10.1016/0092-8674(94)90117-1

Guo, W., Zhang, J., Zhang, N., Xin, M., Peng, H., Hu, Z., Ni, Z., & Du, J. (2015). The Wheat NAC Transcription Factor TaNAC2L Is Regulated at the Transcriptional and Post-Translational Levels and Promotes Heat Stress Tolerance in Transgenic Arabidopsis. *PLOS ONE*, *10*(8), e0135667. https://doi.org/10.1371/journal.pone.0135667

Guo, Y., Mahony, S., & Gifford, D. K. (2012). High Resolution Genome Wide Binding Event Finding and Motif Discovery Reveals Transcription Factor Spatial Binding Constraints. *PLOS Computational Biology*, *8*(8), e1002638. https://doi.org/10.1371/journal.pcbi.1002638

Hachez, C., Veselov, D., Ye, Q., Reinhardt, H., Knipfer, T., Fricke, W., & Chaumont, F. (2012). Short-term control of maize cell and root water permeability through plasma membrane aquaporin isoforms. *Plant, Cell & Environment*, *35*(1), 185-198. https://doi.org/10.1111/j.1365-3040.2011.02429.x

Hao, Y.-J., Song, Q.-X., Chen, H.-W., Zou, H.-F., Wei, W., Kang, X.-S., Ma, B., Zhang, W.-K., Zhang, J.-S., & Chen, S.-Y. (2010). Plant NAC-type transcription factor proteins contain a NARD domain for repression of transcriptional activation. *Planta*, *232*(5), 1033-1043. https://doi.org/10.1007/s00425-010-1238-2

Heger, A., Webber, C., Goodson, M., Ponting, C. P., & Lunter, G. (2013). GAT : A simulation framework for testing the association of genomic intervals. *Bioinformatics*, *29*(16), 2046-2048. https://doi.org/10.1093/bioinformatics/btt343

Hellman, L. M., & Fried, M. G. (2007). Electrophoretic mobility shift assay (EMSA) for detecting protein–nucleic acid interactions. *Nature Protocols*, *2*(8), Article 8. https://doi.org/10.1038/nprot.2007.249

Hook, P. W., & Timp, W. (2023). Beyond assembly : The increasing flexibility of single-molecule sequencing technology. *Nature Reviews Genetics*, 1-15. https://doi.org/10.1038/s41576-023-00600-1

Hoopes, G. M., Hamilton, J. P., Wood, J. C., Esteban, E., Pasha, A., Vaillancourt, B., Provart, N. J., & Buell, C. R. (2019). An updated gene atlas for maize reveals organ-specific and stress-induced genes. *The Plant Journal*, *97*(6), 1154-1167. https://doi.org/10.1111/tpj.14184

Hope, I. A., & Struhl, K. (1986). Functional dissection of a eukaryotic transcriptional activator protein, GCN4 of Yeast. *Cell*, *46*(6), 885-894. https://doi.org/10.1016/0092-8674(86)90070-X

Huang, H., Mizukami, Y., Hu, Y., & Ma, H. (1993). Isolation and characterization of the binding sequences for the product of the Arabidopsis floral homeotic gene AGAMOUS. *Nucleic Acids Research*, *21*(20), 4769-4776. https://doi.org/10.1093/nar/21.20.4769

IPCC. (2023). *AR6 Synthesis Report : Climate Change 2023*. https://www.ipcc.ch/report/ar6/syr/

Ishikawa, F., Suga, S., Uemura, T., Sato, M. H., & Maeshima, M. (2005). Novel type aquaporin SIPs are mainly localized to the ER membrane and show cell-specific expression in Arabidopsis thaliana. *FEBS Letters*, *579*(25), 5814-5820. https://doi.org/10.1016/j.febslet.2005.09.076

Iwafuchi-Doi, M., & Zaret, K. S. (2014). Pioneer transcription factors in cell reprogramming. *Genes & Development*, *28*(24), 2679-2692. https://doi.org/10.1101/gad.253443.114

Jans, D. A., Xiao, C. Y., & Lam, M. H. (2000). Nuclear targeting signal recognition : A key control point in nuclear transport? *BioEssays: News and Reviews in Molecular, Cellular and Developmental Biology*, *22*(6), 532-544. https://doi.org/10.1002/(SICI)1521-1878(200006)22:6<532::AID-BIES6>3.0.CO;2-O

Jensen, M. K., Kjaersgaard, T., Nielsen, M. M., Galberg, P., Petersen, K., O'Shea, C., & Skriver, K. (2010). The *Arabidopsis thaliana* NAC transcription factor family : Structure–function relationships and determinants of ANAC019 stress signalling. *Biochemical Journal*, *426*(2), 183-196. https://doi.org/10.1042/BJ20091234

Jeong, J. S., Park, Y. T., Jung, H., Park, S.-H., & Kim, J.-K. (2009). Rice NAC proteins act as homodimers and heterodimers. *Plant Biotechnology Reports*, *3*(2), 127-134. https://doi.org/10.1007/s11816-009-0081-z

Johanson, U., Karlsson, M., Johansson, I., Gustavsson, S., Sjövall, S., Fraysse, L., Weig, A. R., & Kjellbom, P. (2001). The complete set of genes encoding major intrinsic proteins in Arabidopsis provides a framework for a new nomenclature for major intrinsic proteins in plants. *Plant Physiology*, *126*(4), 1358-1369. https://doi.org/10.1104/pp.126.4.1358

Juven-Gershon, T., Hsu, J.-Y., Theisen, J. W., & Kadonaga, J. T. (2008). The RNA polymerase II core promoter—The gateway to transcription. *Current Opinion in Cell Biology*, *20*(3), 253-259. https://doi.org/10.1016/j.ceb.2008.03.003

K. Flores, J., Kariawasam, R., X. Gimenez, A., Helder, S., Cubeddu, L., Gamsjaeger, R., & F. Ataide, S. (2015). Biophysical Characterisation and Quantification of Nucleic Acid-Protein Interactions : EMSA, MST and SPR. *Current Protein and Peptide Science*, *16*(8), 727-734.

Kalderon, D., Roberts, B. L., Richardson, W. D., & Smith, A. E. (1984). A short amino acid sequence able to specify nuclear location. *Cell*, *39*(3, Part 2), 499-509. https://doi.org/10.1016/0092-8674(84)90457-4

Kammerloher, W., Fischer, U., Piechottka, G. P., & Schäffner, A. R. (1994). Water channels in the plant plasma membrane cloned by immunoselection from a mammalian expression system. *The Plant Journal: For Cell and Molecular Biology*, *6*(2), 187-199. https://doi.org/10.1046/j.1365-313x.1994.6020187.x

Katagiri, F., & Chua, N.-H. (1992). Plant transcription factors : Present knowledge and future challenges. *Trends in Genetics*, *8*(1), 22-27. https://doi.org/10.1016/0168-9525(92)90020-5

Katzen, F. (2007). Gateway(®) recombinational cloning : A biological operating system. *Expert Opinion on Drug Discovery*, *2*(4), 571-589. https://doi.org/10.1517/17460441.2.4.571

Keegan, L., Gill, G., & Ptashne, M. (1986). Separation of DNA Binding from the Transcription-Activating Function of a Eukaryotic Regulatory Protein. *Science*, *231*(4739), 699-704. https://doi.org/10.1126/science.3080805

Kidder, B. L., Hu, G., & Zhao, K. (2011). ChIP-Seq : Technical considerations for obtaining high-quality data. *Nature Immunology*, *12*(10), Article 10. https://doi.org/10.1038/ni.2117

Kim, H. J., Hong, S. H., Kim, Y. W., Lee, I. H., Jun, J. H., Phee, B.-K., Rupak, T., Jeong, H., Lee, Y., Hong, B. S., Nam, H. G., Woo, H. R., & Lim, P. O. (2014). Gene regulatory cascade of senescence-associated NAC transcription factors activated by ETHYLENE-INSENSITIVE2-mediated leaf senescence signalling in Arabidopsis. *Journal of Experimental Botany*, *65*(14), 4023-4036. https://doi.org/10.1093/jxb/eru112

Kim, H. J., Nam, H. G., & Lim, P. O. (2016). Regulatory network of NAC transcription factors in leaf senescence. *Current Opinion in Plant Biology*, *33*, 48-56. https://doi.org/10.1016/j.pbi.2016.06.002

Kimotho, R. N., Baillo, E. H., & Zhang, Z. (2019). Transcription factors involved in abiotic stress responses in Maize (Zea mays L.) and their roles in enhanced productivity in the post genomics era. *PeerJ*, *7*, e7211. https://doi.org/10.7717/peerj.7211

Kleinow, T., Himbert, S., Krenz, B., Jeske, H., & Koncz, C. (2009). NAC domain transcription factor ATAF1 interacts with SNF1-related kinases and silencing of its subfamily causes severe developmental defects in Arabidopsis. *Plant Science*, *177*, 360-370. https://doi.org/10.1016/j.plantsci.2009.06.011

Köster, J., & Rahmann, S. (2012). Snakemake—A scalable bioinformatics workflow engine. *Bioinformatics*, *28*(19), 2520-2522. https://doi.org/10.1093/bioinformatics/bts480

Lalonde, S., Ehrhardt, D. W., Loqué, D., Chen, J., Rhee, S. Y., & Frommer, W. B. (2008). Molecular and cellular approaches for the detection of protein–protein interactions : Latest techniques and current limitations. *The Plant Journal*, *53*(4), 610-635. https://doi.org/10.1111/j.1365-313X.2007.03332.x

Lane, D., Prentki, P., & Chandler, M. (1992). Use of gel retardation to analyze protein-nucleic acid interactions. *Microbiological Reviews*, *56*(4), 509-528. https://doi.org/10.1128/mr.56.4.509-528.1992

Langmead, B., & Salzberg, S. L. (2012). Fast gapped-read alignment with Bowtie 2. *Nature Methods*, *9*(4), Article 4. https://doi.org/10.1038/nmeth.1923

Lenhard, B., Sandelin, A., & Carninci, P. (2012). Metazoan promoters : Emerging characteristics and insights into transcriptional regulation. *Nature Reviews Genetics*, *13*(4), Article 4. https://doi.org/10.1038/nrg3163

Li, J. J., & Herskowitz, I. (1993). Isolation of ORC6, a Component of the Yeast Origin Recognition Complex by a One-Hybrid System. *Science*, *262*(5141), 1870-1874. https://doi.org/10.1126/science.8266075

Li, M., & Huang, S.-S. C. (2022). DNA Affinity Purification Sequencing (DAP-Seq) for Mapping Genome-Wide Transcription Factor Binding Sites in Plants. In A. Bilichak & J.

D. Laurie (Éds.), *Accelerated Breeding of Cereal Crops* (p. 293-303). Springer US. https://doi.org/10.1007/978-1-0716-1526-3_15

Li, S., Wang, L., Zhang, Y., Zhu, G., Zhu, X., Xia, Y., Li, J., Gao, X., Wang, S., Zhang, J., Wuyun, T., & Mo, W. (2021). Genome-Wide Identification and Function of Aquaporin Genes During Dormancy and Sprouting Periods of Kernel-Using Apricot (Prunus armeniaca L.). *Frontiers in Plant Science*, *12*. https://www.frontiersin.org/articles/10.3389/fpls.2021.690040

Lim, P. O., Kim, H. J., & Gil Nam, H. (2007). Leaf Senescence. *Annual Review of Plant Biology*, *58*(1), 115-136. https://doi.org/10.1146/annurev.arplant.57.032905.105316

Liu, G.-S., Li, H.-L., Grierson, D., & Fu, D.-Q. (2022). NAC Transcription Factor Family Regulation of Fruit Ripening and Quality : A Review. *Cells*, *11*(3), Article 3. https://doi.org/10.3390/cells11030525

Liu, H., Song, S., Liu, M., Mu, Y., Li, Y., Xuan, Y., Niu, L., Zhang, H., & Wang, W. (2023). Transcription Factor ZmNAC20 Improves Drought Resistance by Promoting Stomatal Closure and Activating Expression of Stress-Responsive Genes in Maize. *International Journal of Molecular Sciences*, *24*(5), Article 5. https://doi.org/10.3390/ijms24054712

Liu, Y., Wang, C., Li, F., Shen, S., Tyrrell, D. L. J., Le, X. C., & Li, X.-F. (2012). DNase-Mediated Single-Cycle Selection of Aptamers for Proteins Blotted on a Membrane. *Analytical Chemistry*, *84*(18), 7603-7606. https://doi.org/10.1021/ac302047e

Los, G. V., Encell, L. P., McDougall, M. G., Hartzell, D. D., Karassina, N., Zimprich, C., Wood, M. G., Learish, R., Ohana, R. F., Urh, M., Simpson, D., Mendez, J., Zimmerman, K., Otto, P., Vidugiris, G., Zhu, J., Darzins, A., Klaubert, D. H., Bulleit, R. F., & Wood, K. V. (2008). HaloTag : A Novel Protein Labeling Technology for Cell Imaging and Protein Analysis. *ACS Chemical Biology*, *3*(6), 373-382. https://doi.org/10.1021/cb800025k

Lou, X., Qian, J., Xiao, Y., Viel, L., Gerdon, A. E., Lagally, E. T., Atzberger, P., Tarasow, T. M., Heeger, A. J., & Soh, H. T. (2009). Micromagnetic selection of aptamers in microfluidic channels. *Proceedings of the National Academy of Sciences*, *106*(9), 2989-2994. https://doi.org/10.1073/pnas.0813135106

Lu, J., Wu, T., Zhang, B., Liu, S., Song, W., Qiao, J., & Ruan, H. (2021). Types of nuclear localization signals and mechanisms of protein import into the nucleus. *Cell Communication and Signaling*, *19*(1), Article 1. https://doi.org/10.1186/s12964-021-00741-y

Lu, M., Ying, S., Zhang, D.-F., Shi, Y.-S., Song, Y.-C., Wang, T.-Y., & Li, Y. (2012). A maize stress-responsive NAC transcription factor, ZmSNAC1, confers enhanced tolerance to dehydration in transgenic Arabidopsis. *Plant Cell Reports*, *31*(9), 1701-1711. https://doi.org/10.1007/s00299-012-1284-2

Luo, P., Chen, Y., Rong, K., Lu, Y., Wang, N., Xu, Z., Pang, B., Zhou, D., Weng, J., Li, M., Zhang, D., Yong, H., Han, J., Zhou, Z., Gao, W., Hao, Z., & Li, X. (2022). ZmSNAC13, a maize NAC transcription factor conferring enhanced resistance to multiple abiotic stresses in transgenic Arabidopsis. *Plant Physiology and Biochemistry*, *170*, 160-170. https://doi.org/10.1016/j.plaphy.2021.11.032

Machanick, P., & Bailey, T. L. (2011). MEME-ChIP : Motif analysis of large DNA datasets. *Bioinformatics (Oxford, England)*, *27*(12), 1696-1697.

https://doi.org/10.1093/bioinformatics/btr189

Maistriaux, L. (2021). *Genetic variability of the expression of plasma membrane aquaporins in maize leaves : From eQTLs to characterization of cis- and trans-acting regulatory factors* [UCL - Université Catholique de Louvain]. https://dial.uclouvain.be/pr/boreal/fr/object/boreal%3A242580

Mardis, E. R. (2007). ChIP-seq : Welcome to the new frontier. *Nature Methods*, *4*(8), 613-614. https://doi.org/10.1038/nmeth0807-613

Mathew, I. E., & Agarwal, P. (2018). May the Fittest Protein Evolve : Favoring the Plant-Specific Origin and Expansion of NAC Transcription Factors. *BioEssays*, *40*(8), 1800018. https://doi.org/10.1002/bies.201800018

Moshelion, M., Hachez, C., Ye, Q., Cavez, D., Bajji, M., Jung, R., & Chaumont, F. (2009). Membrane water permeability and aquaporin expression increase during growth of maize suspension cultured cells. *Plant, Cell & Environment*, *32*(10), 1334-1345. https://doi.org/10.1111/j.1365-3040.2009.02001.x

Mukherjee, S., Berger, M. F., Jona, G., Wang, X. S., Muzzey, D., Snyder, M., Young, R. A., & Bulyk, M. L. (2004). Rapid analysis of the DNA-binding specificities of transcription factors with DNA microarrays. *Nature Genetics*, *36*(12), Article 12. https://doi.org/10.1038/ng1473

Nakashima, K., Takasaki, H., Mizoi, J., Shinozaki, K., & Yamaguchi-Shinozaki, K. (2012). NAC transcription factors in plant abiotic stress responses. *Biochimica et Biophysica Acta (BBA) - Gene Regulatory Mechanisms*, *1819*(2), 97-103. https://doi.org/10.1016/j.bbagrm.2011.10.005

Nole-Wilson, S., & Krizek, B. A. (2000). DNA binding properties of the Arabidopsis floral development protein AINTEGUMENTA. *Nucleic Acids Research*, *28*(21), 4076-4082. https://doi.org/10.1093/nar/28.21.4076

Nuruzzaman, M., Manimekalai, R., Sharoni, A. M., Satoh, K., Kondoh, H., Ooka, H., & Kikuchi, S. (2010). Genome-wide analysis of NAC transcription factor family in rice. *Gene*, *465*(1), 30-44. https://doi.org/10.1016/j.gene.2010.06.008

Oliphant, A. R., Brandl, C. J., & Struhl, K. (1989). Defining the Sequence Specificity of DNA-Binding Proteins by Selecting Binding Sites from Random-Sequence Oligonucleotides : Analysis of Yeast GCN4 Protein. *Molecular and Cellular Biology*, *9*(7), 2944-2949. https://doi.org/10.1128/mcb.9.7.2944-2949.1989

Olsen, A. N., Ernst, H. A., Leggio, L. L., & Skriver, K. (2005). NAC transcription factors : Structurally distinct, functionally diverse. *Trends in Plant Science*, *10*(2), 79-87. https://doi.org/10.1016/j.tplants.2004.12.010

O'Malley, R. C., Huang, S.-S. C., Song, L., Lewsey, M. G., Bartlett, A., Nery, J. R., Galli, M., Gallavotti, A., & Ecker, J. R. (2016). Cistrome and Epicistrome Features Shape the Regulatory DNA Landscape. *Cell*, *165*(5), 1280-1292. https://doi.org/10.1016/j.cell.2016.04.038

Ouwerkerk, P. B. F., & Meijer, A. H. (2001). Yeast One-Hybrid Screening for DNA-Protein Interactions. *Current Protocols in Molecular Biology*, *55*(1), 12.12.1-12.12.12. https://doi.org/10.1002/0471142727.mb1212s55

Pabo, C. O., & Sauer, R. T. (1992). TRANSCRIPTION FACTORS : Structural Families and Principles of DNA Recognition. *Annual Review of Biochemistry*, *61*(1), 1053-1095.

https://doi.org/10.1146/annurev.bi.61.070192.005201

Pei, H., Ma, N., Tian, J., Luo, J., Chen, J., Li, J., Zheng, Y., Chen, X., Fei, Z., & Gao, J. (2013). An NAC Transcription Factor Controls Ethylene-Regulated Cell Expansion in Flower Petals. *Plant Physiology*, *163*(2), 775-791. https://doi.org/10.1104/pp.113.223388

Peng, X., Zhao, Y., Li, X., Wu, M., Chai, W., Sheng, L., Wang, Y., Dong, Q., Jiang, H., & Cheng, B. (2015). Genomewide identification, classification and analysis of NAC type gene family in maize. *Journal of Genetics*, *94*(3), 377-390. https://doi.org/10.1007/s12041-015-0526-9

Pickard, W. F. (2008). Modelling the swelling assay for aquaporin expression. *Journal of Mathematical Biology*, *57*(6), 883-903. https://doi.org/10.1007/s00285-008-0196-9

Podzimska-Sroka, D., O'Shea, C., Gregersen, P. L., & Skriver, K. (2015). NAC Transcription Factors in Senescence : From Molecular Structure to Function in Crops. *Plants*, *4*(3), Article 3. https://doi.org/10.3390/plants4030412

Puranik, S., Sahu, P. P., Srivastava, P. S., & Prasad, M. (2012). NAC proteins : Regulation and role in stress tolerance. *Trends in Plant Science*, *17*(6), 369-381. https://doi.org/10.1016/j.tplants.2012.02.004

Ramírez, F., Dündar, F., Diehl, S., Grüning, B. A., & Manke, T. (2014). deepTools : A flexible platform for exploring deep-sequencing data. *Nucleic Acids Research*, *42*(Web Server issue), W187-191. https://doi.org/10.1093/nar/gku365

Reed, J., & Osbourn, A. (2018). Engineering terpenoid production through transient expression in Nicotiana benthamiana. *Plant Cell Reports*, *37*(10), 1431-1441. https://doi.org/10.1007/s00299-018-2296-3

Ren, Y., Huang, Z., Jiang, H., Wang, Z., Wu, F., Xiong, Y., & Yao, J. (2021). A heat stress responsive NAC transcription factor heterodimer plays key roles in rice grain filling. *Journal of Experimental Botany*, *72*(8), 2947-2964. https://doi.org/10.1093/jxb/erab027

Salika, R., & Riffat, J. (2021). Abiotic stress responses in maize : A review. *Acta Physiologiae Plantarum*, *43*(9), 130. https://doi.org/10.1007/s11738-021-03296-0

Seo, M., Lei, L., & Egli, M. (2019). Label-Free Electrophoretic Mobility Shift Assay (EMSA) for Measuring Dissociation Constants of Protein-RNA Complexes. *Current Protocols in Nucleic Acid Chemistry*, *76*(1), e70. https://doi.org/10.1002/cpnc.70

Seo, P. J., Kim, S.-G., & Park, C.-M. (2008). Membrane-bound transcription factors in plants. *Trends in Plant Science*, *13*(10), 550-556. https://doi.org/10.1016/j.tplants.2008.06.008

Sewell, J. A., & Fuxman Bass, J. I. (2018). Options and Considerations When Using a Yeast One-Hybrid System. In L. Oñate-Sánchez (Éd.), *Two-Hybrid Systems : Methods and Protocols* (p. 119-130). Springer. https://doi.org/10.1007/978-1-4939-7871-7_8

Shen, H., Yin, Y., Chen, F., Xu, Y., & Dixon, R. A. (2009). A Bioinformatic Analysis of NAC Genes for Plant Cell Wall Development in Relation to Lignocellulosic Bioenergy Production. *BioEnergy Research*, *2*(4), 217-232. https://doi.org/10.1007/s12155-009-9047-9

Sheridan, W. F. (1975). Growth of corn cells in culture. *J Cell Biol*.

Sheridan, W. F. (1982). Black Mexican sweet corn : Its use for tissue cultures. *FAO of the UN*

Shibuya, K., Shimizu, K., Niki, T., & Ichimura, K. (2014). Identification of a NAC transcription factor, EPHEMERAL1, that controls petal senescence in Japanese morning glory. *The Plant Journal*, *79*(6), 1044-1051. https://doi.org/10.1111/tpj.12605

Shiriga, K., Sharma, R., Kumar, K., Yadav, S. K., Hossain, F., & Thirunavukkarasu, N. (2014). Genome-wide identification and expression pattern of drought-responsive members of the NAC family in maize. *Meta Gene*, *2*, 407-417. https://doi.org/10.1016/j.mgene.2014.05.001

Sieweke, M. (2000). Detection of transcription factor partners with a yeast one hybrid screen. *Methods in Molecular Biology (Clifton, N.J.)*, *130*, 59-77. https://doi.org/10.1385/1-59259-686-x:59

Singh, S., Koyama, H., Bhati, K. K., & Alok, A. (2021). The biotechnological importance of the plant-specific NAC transcription factor family in crop improvement. *Journal of Plant Research*, *134*(3), 475-495. https://doi.org/10.1007/s10265-021-01270-y

Skene, P. J., & Henikoff, S. (2017a). An efficient targeted nuclease strategy for high-resolution mapping of DNA binding sites. *eLife*, *6*, e21856. https://doi.org/10.7554/eLife.21856

Skene, P. J., & Henikoff, S. (2017b). *CUT&RUN : Targeted in situ genome-wide profiling with high efficiency for low cell numbers* (p. 193219). bioRxiv. https://doi.org/10.1101/193219

Sönmezer, C., Kleinendorst, R., Imanci, D., Barzaghi, G., Villacorta, L., Schübeler, D., Benes, V., Molina, N., & Krebs, A. R. (2021). Molecular Co-occupancy Identifies Transcription Factor Binding Cooperativity In Vivo. *Molecular Cell*, *81*(2), 255-267.e6. https://doi.org/10.1016/j.molcel.2020.11.015

Souer, E., van Houwelingen, A., Kloos, D., Mol, J., & Koes, R. (1996). The No Apical Meristem Gene of Petunia Is Required for Pattern Formation in Embryos and Flowers and Is Expressed at Meristem and Primordia Boundaries. *Cell*, *85*(2), 159-170. https://doi.org/10.1016/S0092-8674(00)81093-4

Spitz, F., & Furlong, E. E. M. (2012). Transcription factors : From enhancer binding to developmental control. *Nature Reviews Genetics*, *13*(9), Article 9. https://doi.org/10.1038/nrg3207

Steiner, S., & Pfannschmidt, T. (2009). Fluorescence-based Electrophoretic Mobility Shift Assay in the Analysis of DNA-binding Proteins. In T. Pfannschmidt (Éd.), *Plant Signal Transduction : Methods and Protocols* (p. 273-289). Humana Press. https://doi.org/10.1007/978-1-59745-289-2_18

Stelpflug, S. C., Sekhon, R. S., Vaillancourt, B., Hirsch, C. N., Buell, C. R., de Leon, N., & Kaeppler, S. M. (2016). An Expanded Maize Gene Expression Atlas based on RNA Sequencing and its Use to Explore Root Development. *The Plant Genome*, *9*(1), plantgenome2015.04.0025. https://doi.org/10.3835/plantgenome2015.04.0025

Steudle, E., & Peterson, C. A. (1998). How does water get through roots? *Journal of Experimental Botany*, *49*(322), 775-788. https://doi.org/10.1093/jxb/49.322.775

Su, Y., Liu, Z., Sun, J., Wu, C., Li, Y., Zhang, C., & Zhao, L. (2022). Genome-Wide Identification of Maize Aquaporin and Functional Analysis During Seed Germination and Seedling Establishment. *Frontiers in Plant Science*, *13*. https://www.frontiersin.org/articles/10.3389/fpls.2022.831916

Teirlinckx, E. (2020). *Characterization of a NAC transcription factor putatively influencing ZmPIP2;5 expression*.

Tran, L.-S. P., Nakashima, K., Sakuma, Y., Osakabe, Y., Qin, F., Simpson, S. D., Maruyama, K., Fujita, Y., Shinozaki, K., & Yamaguchi-Shinozaki, K. (2007). Co-expression of the stress-inducible zinc finger homeodomain ZFHD1 and NAC transcription factors enhances expression of the ERD1 gene in Arabidopsis. *The Plant Journal*, *49*(1), 46-63. https://doi.org/10.1111/j.1365-313X.2006.02932.x

Tran, L.-S. P., Quach, T. N., Guttikonda, S. K., Aldrich, D. L., Kumar, R., Neelakandan, A., Valliyodan, B., & Nguyen, H. T. (2009). Molecular characterization of stress-inducible GmNAC genes in soybean. *Molecular Genetics and Genomics*, *281*(6), 647-664. https://doi.org/10.1007/s00438-009-0436-8

Tuerk, C., & Gold, L. (1990). Systematic Evolution of Ligands by Exponential Enrichment : RNA Ligands to Bacteriophage T4 DNA Polymerase. *Science*, *249*(4968), 505-510. https://doi.org/10.1126/science.2200121

Uehlein, N., Kai, L., & Kaldenhoff, R. (2017). Plant Aquaporins and CO2. In F. Chaumont & S. D. Tyerman (Éds.), *Plant Aquaporins : From Transport to Signaling* (p. 255-265). Springer International Publishing. https://doi.org/10.1007/978-3-319-49395-4_12

Uhrig, J. F. (2006). Protein interaction networks in plants. *Planta*, *224*(4), 771-781. https://doi.org/10.1007/s00425-006-0260-x

Van Bel, M., Diels, T., Vancaester, E., Kreft, L., Botzki, A., Van de Peer, Y., Coppens, F., & Vandepoele, K. (2018). PLAZA 4.0 : An integrative resource for functional, evolutionary and comparative plant genomics. *Nucleic Acids Research*, *46*(D1), D1190-D1196. https://doi.org/10.1093/nar/gkx1002

Varma, A., Padh, H., & Shrivastava, N. (2007). Plant genomic DNA isolation : An art or a science. *Biotechnology Journal*, *2*(3), 386-392. https://doi.org/10.1002/biot.200600195

Vierstra, J., & Stamatoyannopoulos, J. A. (2016). Genomic footprinting. *Nature Methods*, *13*(3), Article 3. https://doi.org/10.1038/nmeth.3768

Viola, I. L., & Gonzalez, D. H. (2011). Footprinting and Missing Nucleoside Analysis of Transcription Factor–DNA Complexes. In L. Yuan & S. E. Perry (Éds.), *Plant Transcription Factors : Methods and Protocols* (p. 259-275). Humana Press. https://doi.org/10.1007/978-1-61779-154-3_15

Voitsik, A.-M., Muench, S., Deising, H. B., & Voll, L. M. (2013). Two recently duplicated maize NAC transcription factor paralogs are induced in response to Colletotrichum graminicola infection. *BMC Plant Biology*, *13*(1), Article 1. https://doi.org/10.1186/1471-2229-13-85

Walter, J., Dever, C. A., & Biggin, M. D. (1994). Two homeo domain proteins bind with similar specificity to a wide range of DNA sites in Drosophila embryos. *Genes & Development*, *8*(14), 1678-1692. https://doi.org/10.1101/gad.8.14.1678

Wang, B., Zheng, J., Liu, Y., Wang, J., & Wang, G. (2012). Cloning and characterization of the stress-induced bZIP gene ZmbZIP60 from maize. *Molecular Biology Reports*, *39*(5), 6319-6327. https://doi.org/10.1007/s11033-012-1453-y

Wang, B., Zhong, Z., Wang, X., Han, X., Yu, D., Wang, C., Song, W., Zheng, X., Chen, C., & Zhang, Y. (2020). Knockout of the OsNAC006 Transcription Factor Causes

Drought and Heat Sensitivity in Rice. *International Journal of Molecular Sciences*, *21*(7), Article 7. https://doi.org/10.3390/ijms21072288

Wang, G., Yuan, Z., Zhang, P., Liu, Z., Wang, T., & Wei, L. (2020). Genome-wide analysis of NAC transcription factor family in maize under drought stress and rewatering. *Physiology and Molecular Biology of Plants*, *26*(4), 705-717. https://doi.org/10.1007/s12298-020-00770-w

Wang, G., Zhang, S., Ma, X., Wang, Y., Kong, F., & Meng, Q. (2016). A stress-associated NAC transcription factor (SlNAC35) from tomato plays a positive role in biotic and abiotic stresses. *Physiologia Plantarum*, *158*(1), 45-64. https://doi.org/10.1111/ppl.12444

Wang, R., Zhang, Y., Wang, C., Wang, Y.-C., & Wang, L.-Q. (2021). ThNAC12 from Tamarix hispida directly regulates ThPIP2;5 to enhance salt tolerance by modulating reactive oxygen species. *Plant Physiology and Biochemistry*, *163*, 27-35. https://doi.org/10.1016/j.plaphy.2021.03.042

Wang, Y., Li, R., Li, D., Jia, X., Zhou, D., Li, J., Lyi, S. M., Hou, S., Huang, Y., Kochian, L. V., & Liu, J. (2017). NIP1;2 is a plasma membrane-localized transporter mediating aluminum uptake, translocation, and tolerance in Arabidopsis. *Proceedings of the National Academy of Sciences*, *114*(19), 5047-5052. https://doi.org/10.1073/pnas.1618557114

Weber, B., Zicola, J., Oka, R., & Stam, M. (2016). Plant Enhancers : A Call for Discovery. *Trends in Plant Science*, *21*(11), 974-987. https://doi.org/10.1016/j.tplants.2016.07.013

Welcome to MaizeGDB. (s. d.). Consulté 8 mai 2023, à l'adresse https://www.maizegdb.org/

Welner, D. H., Deeba, F., Lo Leggio, L., & Skriver, K. (2016). Chapter 13 - NAC Transcription Factors : From Structure to Function in Stress-Associated Networks. In D. H. Gonzalez (Éd.), *Plant Transcription Factors* (p. 199-212). Academic Press. https://doi.org/10.1016/B978-0-12-800854-6.00013-0

Welner, D. H., Lindemose, S., Grossmann, J. G., Møllegaard, N. E., Olsen, A. N., Helgstrand, C., Skriver, K., & Lo Leggio, L. (2012). DNA binding by the plant-specific NAC transcription factors in crystal and solution : A firm link to WRKY and GCM transcription factors. *Biochemical Journal*, *444*(3), 395-404. Scopus. https://doi.org/10.1042/BJ20111742

Winter, D., Vinegar, B., Nahal, H., Ammar, R., Wilson, G. V., & Provart, N. J. (2007). An "Electronic Fluorescent Pictograph" Browser for Exploring and Analyzing Large-Scale Biological Data Sets. *PLOS ONE*, *2*(8), e718. https://doi.org/10.1371/journal.pone.0000718

Wu, J., Smith, L. T., Plass, C., & Huang, T. H.-M. (2006). ChIP-chip comes of age for genome-wide functional analysis. *Cancer Research*, *66*(14), 6899-6902. https://doi.org/10.1158/0008-5472.CAN-06-0276

Wu, Y. X., & Kwon, Y. J. (2016). Aptamers : The "evolution" of SELEX. *Methods*, *106*, 21-28. https://doi.org/10.1016/j.ymeth.2016.04.020

Xi, Y., Ling, Q., Zhou, Y., Liu, X., & Qian, Y. (2022). ZmNAC074, a maize stress-responsive NAC transcription factor, confers heat stress tolerance in transgenic Arabidopsis. *Frontiers in Plant Science*, *13*, 986628.

https://doi.org/10.3389/fpls.2022.986628

Yamaguchi, M., Ohtani, M., Mitsuda, N., Kubo, M., Ohme-Takagi, M., Fukuda, H., & Demura, T. (2010). VND-INTERACTING2, a NAC Domain Transcription Factor, Negatively Regulates Xylem Vessel Formation in Arabidopsis. *The Plant Cell*, *22*(4), 1249-1263. https://doi.org/10.1105/tpc.108.064048

Yamasaki, K., Kigawa, T., Watanabe, S., Inoue, M., Yamasaki, T., Seki, M., Shinozaki, K., & Yokoyama, S. (2012). Structural Basis for Sequence-specific DNA Recognition by an Arabidopsis WRKY Transcription Factor*. *Journal of Biological Chemistry*, *287*(10), 7683-7691. https://doi.org/10.1074/jbc.M111.279844

Yaneff, A., Vitali, V., & Amodeo, G. (2015). PIP1 aquaporins : Intrinsic water channels or PIP2 aquaporin modulators? *FEBS Letters*, *589*(23), 3508-3515. https://doi.org/10.1016/j.febslet.2015.10.018

Yang, S., Zhao, D., Li, M., Cai, D., Zhang, Y., Ding, D., Yao, L., & Duan, P. (2022). Conserved Zma-miR164 family is responsible for maize heterosis by negatively regulating NAC transcription factor during internode elongation. *South African Journal of Botany*, *150*, 806-812. https://doi.org/10.1016/j.sajb.2022.05.049

Yazaki, J., Galli, M., Kim, A. Y., Nito, K., Aleman, F., Chang, K. N., Carvunis, A.-R., Quan, R., Nguyen, H., Song, L., Alvarez, J. M., Huang, S. C., Chen, H., Ramachandran, N., Altmann, S., Gutiérrez, R. A., Hill, D. E., Schroeder, J. I., Chory, J., … Ecker, J. R. (2016). Mapping transcription factor interactome networks using HaloTag protein arrays. *Proceedings of the National Academy of Sciences of the United States of America*, *113*(29), E4238-E4247. https://doi.org/10.1073/pnas.1603229113

Yuan, X., Wang, H., Cai, J., Li, D., & Song, F. (2019). NAC transcription factors in plant immunity. *Phytopathology Research*, *1*(1), 3. https://doi.org/10.1186/s42483-018-0008-0

Yuan, X., Zhao, Q., Xu, J., Yu, J., Zhu, D., & Li, H. (2023). *The Nac Transcription Factor Zmnac132 Regulates Leaf Senescence and Male Fertility in Maize* (SSRN Scholarly Paper Nº 4374093). https://doi.org/10.2139/ssrn.4374093

Zhang, Y., Gao, P., & Yuan, J. S. (2010). Plant Protein-Protein Interaction Network and Interactome. *Current Genomics*, *11*(1), 40-46. https://doi.org/10.2174/138920210790218016

Zhang, Z., Dong, J., Ji, C., Wu, Y., & Messing, J. (2019). NAC-type transcription factors regulate accumulation of starch and protein in maize seeds. *Proceedings of the National Academy of Sciences*, *116*(23), 11223-11228. https://doi.org/10.1073/pnas.1904995116

Zhang, Z., Yang, J., & Wu, Y. (2015). Transcriptional Regulation of Zein Gene Expression in Maize through the Additive and Synergistic Action of opaque2, Prolamine-Box Binding Factor, and O2 Heterodimerizing Proteins. *The Plant Cell*, *27*(4), 1162-1172. https://doi.org/10.1105/tpc.15.00035

Zhao, L., Zhao, K. Q., Hurst, R., Slater, M. R., Acton, T. B., Swapna, G. V. T., Shastry, R., Kornhaber, G. J., & Montelione, G. T. (2010). Engineering of a wheat germ expression system to provide compatibility with a high throughput pET-based cloning platform. *Journal of Structural and Functional Genomics*, *11*(3), 201-209. https://doi.org/10.1007/s10969-010-9093-8

Zheng, X., Chen, B., Lu, G., & Han, B. (2009). Overexpression of a NAC transcription factor enhances rice drought and salt tolerance. *Biochemical and Biophysical Research*

Communications, *379*(4), 985-989. https://doi.org/10.1016/j.bbrc.2008.12.163

Zhu, Q., Zou, J., Zhu, M., Liu, Z., Feng, P., Fan, G., Wang, W., & Liao, H. (2014). In silico analysis on structure and DNA binding mode of AtNAC1, a NAC transcription factor from Arabidopsis thaliana. *Journal of Molecular Modeling*, *20*(3). Scopus. https://doi.org/10.1007/s00894-014-2117-8

Zwiazek, J. J., Xu, H., Tan, X., Navarro-Ródenas, A., & Morte, A. (2017). Significance of oxygen transport through aquaporins. *Scientific Reports*, *7*(1), Article 1. https://doi.org/10.1038/srep40411

Characterization of the ZmNAC24 transcription factor using DAP-seq and an over-expressing cell line

Jean Fontaine

Maize is one of the world's most important crops used for animal feed, human food and non-food applications. As climate change progresses, we are observing an increase in abiotic stresses on ecosystems and organisms. Regulation of water uptake and movement in plants are essential for their physiology, especially in case of drought stress, and these processes depend on the activity of aquaporins. The abundance of these water channels in the cell membranes is primarily dependent on gene expression and therefore on transcription factors (TFs). The NAC TF family play roles in plant responses to abiotic stresses but also in development and growth. We previously identified ZmNAC24 as a TF controlling the expression of *ZmPIP2;5* and *ZmPIP2;9* aquaporin genes, but little more is known about it.

In order to identify other NAC24 target genes and its binding motifs, we set up a DNA Affinity Purification sequencing approach using NAC24 protein and maize root gDNA fragments. We adapted and optimized different steps of the protocol, and succeeded in obtaining gDNA fragments that bind to NAC24. These fragments were sent for sequencing. In addition, we prepare genetic constructs to express tagged NAC24 together with the fluorescent mCherry marker in maize BMS suspension cells. These cells were transformed and fluorescent calli were obtained. These cells lines will be used for a NAC24 ChIP-seq analysis and other functional studies.

UNIVERSITÉ CATHOLIQUE DE LOUVAIN
Faculté des bioingénieurs
Croix du Sud, 2 bte L7.05.01, 1348 Louvain-la-Neuve, Belgique | **www.uclouvain.be/agro**